nature reviews materials

https://doi.org/10.1038/s41578-024-00652-7

Review article

Check for updates

Designing organic mixed conductors for electrochemical transistor applications

Yazhou Wang [1,2], Shofarul Wustoni[1,2], Jokubas Surgailis[1], Yizhou Zhong[1], Anil Koklu[1] & Sahika Inal [1]

Abstract

The organic electrochemical transistor (OECT) has emerged as the core component of specialized bioelectronic technologies, such as neural interfaces and sensors of disease biomarkers. At the heart of the OECT is its channel, made of an organic mixed ionic–electronic conductor (OMIEC). The chemical structure of the OMIEC governs the electronic, optical and mechanical traits of OECT, with even subtle structural tweaks leading to sizeable functional disparities. In this Review, we summarize the recent progress in OECT device development while underscoring the critical role of OMIEC selection in steering diverse applications. Our narrative charts the milestones in materials exploration, tracing the evolution of the field in parallel with polymer chemistry breakthroughs. We emphasize how materials design has enabled new device operation mechanisms by adding features such as biocompatibility, stretchability, stimuli response and memory retention to OMIECs. We also highlight the obstacles that must be surmounted to translate OECT-based devices from laboratory instruments into tangible real-world technologies.

Sections

[1]Organic Bioelectronics Laboratory, Biological and Environmental Science and Engineering (BESE) Division, King Abdullah University of Science and Technology (KAUST), Thuwal, Saudi Arabia. [2]These authors contributed equally: Yazhou Wang, Shofarul Wustoni. e-mail: sahika.inal@kaust.edu.sa

Introduction

In the biotic world, most events (such as cellular signalling and molecular and ion transport) involve movements of ionic charges and biomolecular recognition. The species involved are charged and under constant change. These cellular events lead to local transient changes in ionic charge distribution, which can be monitored with a device wired to translate ionic signals into electronic ones, coupling the realms of electronics and the ion-dominated biological milieu. Among a plethora of bioelectronics devices, the organic electrochemical transistor (OECT) has been at the forefront[1]. The OECT is a transistor that provides power gain, and its primary component is an organic mixed ionic–electronic conductor (OMIEC) film. This film is used in the channel in contact with an electrolyte, which can be the biological fluid itself. OMIECs are typically amphiphilic conjugated polymers capable of simultaneously transporting electronic and ionic charges through their bulk[2].

Because these electronic and ionic charge species are coupled, an intrinsic transduction mechanism is generated, wherein ionic signals affect the electrical conductivity. This coupling, extending throughout the entire OMIEC channel, translates into a remarkably high transconductance (g_m) – given that the charges can transport across the channel. The high g_m of the OECT allows weak biological ionic signals to be converted into large current changes, turning these devices into very powerful sensors[3]. The g_m is, therefore, a direct outcome of the three-dimensional interplay of ionic and electronic charges intrinsic to this specific materials class, underscoring the foundation of the OECT technology. Yet, mixed conduction is not the sole property that OMIECs possess[4]. With the use of OMIECs that have been chemically tuned to possess multi-functionality, OECTs can become more than amplifying transducers or switches.

Through a modification of backbone chemical structure or side chain engineering, OMIECs can attain various values of mobility, capacitance, and oxidation and reduction onsets, and they gain reactivity towards chemical species, the capability to recognize biomarkers, or the ability to retain charge, with each property becoming the enabler of a particular application. For instance, the compatibility of OMIEC films with various biological environments (that is, chemical stability and nontoxicity) permits OECTs to interface directly with living systems, allowing for multiple forms of diagnostics, even in unconventional geometries. These applications span from in vivo neural signal recordings to continuous monitoring of in vitro tissue integrity, and from detecting metabolites to identifying disease biomarkers in bodily fluids such as sweat or the brain[5–8]. The ability to access and store a large density of charge states with voltage modulation allows the use of OECTs within the realm of memory and neuromorphic-related applications[9,10]. With control over the location of the penetrating ions inside the complex microstructure of the channel, OECTs can display short-term or long-term potentiation and depression. It is even possible to mimic the function of a neuron with an OECT, as the operation principle of both relies on ion-modulated spiking, enabling organic artificial neural circuits[11–14].

OMIECs can adopt various forms and geometries, ranging from traditional thin films to fibre-based textile electronics and microporous scaffolds[15,16], and can be patterned on different substrates, as they are compatible with different fabrication methods[17]. OMIECs can even be chemically polymerized inside a living tissue, a step towards generating polymeric electrodes embedded in the tissue in the absence of rigid substrate carriers[18]. Their compatibility with conventional printing methods, as well as digitally enabled direct-write techniques, makes the OECT fabrication simple and cost-effective and enables large-scale production of arrays[17,19].

One property often recognized for the majority of polymeric OMIECs is their softness[20], attributed to the inclusion of polar side chains that assemble in less regular and crystalline domains compared with traditional alkyl side chains[21]. Their low Young modulus, which decreases further as the film swells in an aqueous medium, allows them to match the mechanical properties of soft biological tissue, an advantage when the channel is designed to be in direct contact with the tissue. They can also be programmed to stretch with the underlying substrate, rendering OECTs popular in wearable formats and robotics[22,23]. Moreover, OMIECs can absorb light and photogenerate electronic charges. Using light as the secondary input increases the already high gain of the OECT by at least 20 times, which can help construct sensors with record-high sensitivities[24]. Devices integrating such light-responsive OMIECs are promising for light-controlled logic gates or artificial electronic retinas[24]. By rendering the same materials stretchable, light-gated OECTs can become powerful wearable photodetectors.

OMIECs offer a rich chemical design space, in which not only the backbone units but also the side chains govern their properties. The ability to tune OMIEC function through synthesis enables them to be custom-made for targeted OECT applications. Thus, it is imperative to understand the intricate interplay between device functionality and materials chemistry. In this Review, we aim to contribute to this relationship by taking a deep dive into active OECT materials and the operational principles that underlie their functionality. We first provide molecular design rules for making OMIEC materials, characterized by their mixed charge transport performance. We then overview strategies to develop OMIECs for biosensors, neuromorphic computing and logic circuits, which require them to have functions such as high charge mobility, ambipolarity, ionic charge retention, surface reactivity, photoactivity or stretchability. Finally, we present our insights into the prevailing challenges and future prospects in OECT channel material evolution.

Operation of OECTs

The OECT has a typical three-terminal transistor structure with gate, source and drain electrodes (Fig. 1a). An OMIEC forms the semiconducting channel between the source and drain electrodes, and an ionically conducting medium, such as an aqueous electrolyte, links the channel to the gate. A voltage applied between the gate and source terminals (V_{GS}) orchestrates the movement of ions in and out of the channel, modulating the electronic charge carrier density in the bulk of the film and, hence, the channel conductivity. The OECT's operation in ion-containing media, thus, hinges on the interplay between electrolyte ions and the conjugated polymer backbone, and this defining characteristic of the OECT stems from the channel's ion permeability (Box 1). In contrast to constraining ionic-electronic charge coupling to a two-dimensional channel–electrolyte interface as observed in field-effect transistors, the accumulation of charges throughout the entire volume of the OMIEC leads to very large current changes in the OECT channel under the same sub-volt biasing conditions. The miscibility of a particular ion within the OMIEC is governed by the film's chemical structure and physical properties. Achieving ionic-electronic coupling at accessible potentials requires engineering the OMIEC energetics by incorporating electron-rich and electron-deficient moieties.

The amount of electronic and ionic charge couples in the OMIEC can be quantified by measuring its volumetric capacitance (C^*),

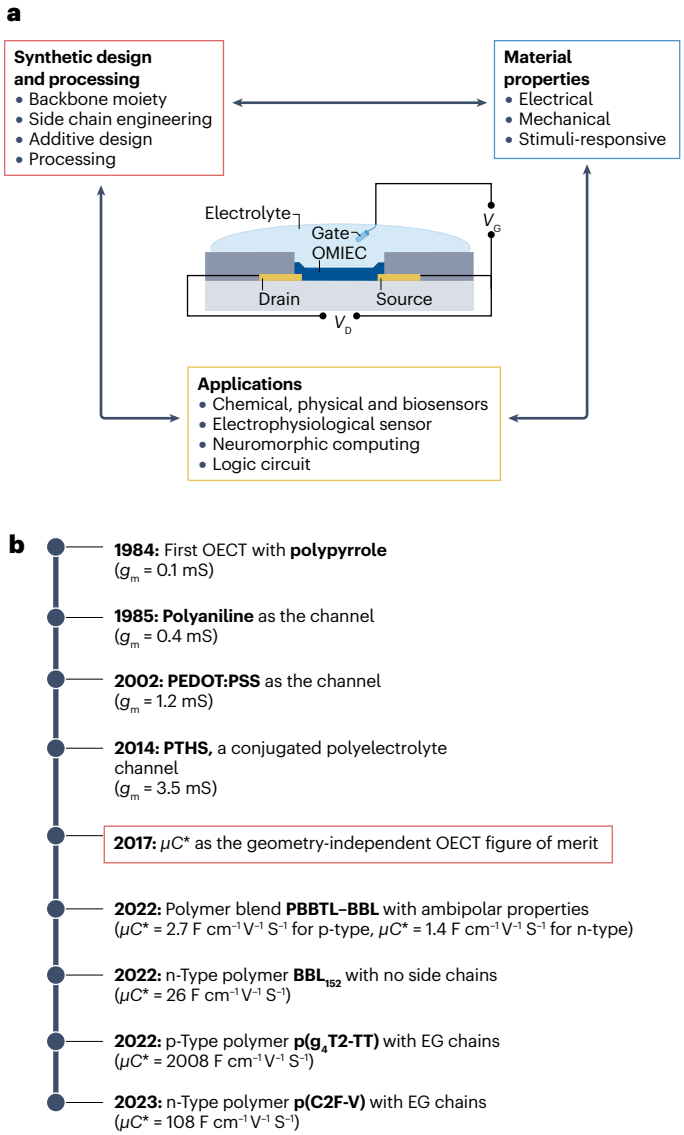

Fig. 1 | Operation and history of OECTs. a, The synthetic design controls the properties of organic mixed ionic–electronic conductors (OMIECs), which enable particular applications. **b**, Timeline of the evolution of organic electrochemical transistor (OECT) channel materials. BBL, poly(benzimidazobenzophenanthroline); EG, ethylene glycol; g_m, transconductance; PEDOT:PSS, poly(3,4-ethylenedioxythiophene):poly(styrene sulfonate); PTHS, poly(6[thiophene-3-yl] hexane-1-sulfonate) tetrabutylammonium; T2, bithiophene; TT, thienothiophene; V_D, drain voltage; V_G, gate voltage.

expressed in farads per cubic centimetre (F cm^{-3}). Once the charges are coupled, a voltage applied between the source and drain contacts (V_{DS}) propels them across the channel towards the respective terminal. The ease with which the charges move across the channel is determined by their mobility (μ_{OECT})[25]. Both C^* and μ_{OECT} are material properties inherent to the OMIEC, and they collectively affect the g_m of the device[26–28]. However, high g_m without a fast response may not be meaningful in applications that require OECTs to process information or detect rapid biological events in real-time. It is the mobility of both ions and electrons that determines how fast the device will respond to ionic fluxes in the electrolyte (or the V_{GS} applied). Making smaller channels can increase the switching speed at the cost of the device g_m. A creative approach to bolstering both properties, without a substantial trade-off, involves trapping ions within the film prior to biasing[8]. A recent stride in the processing of OMIECs is the advent of the vertical OECT design[29,30]. This innovation upholds fast switching speeds and could broaden the potential applications of the device.

While C^* and μ_{OECT} are material properties that impact device output and transient characteristics, for each OMIEC, they vary with respect to the electrolyte (but also the type of gate electrode) used. This is because ionic–electronic charge interactions occur over the entire volume of the film; hence, the ions and solvent molecules become a part of the OMIEC. Conversely, the gate electrode influences the voltage threshold at which ion injection or ejection commences. For each application, there may be a different gate electrode or electrolyte requirement; therefore, while selecting the OMIEC, it is important to evaluate the device functionality in the targeted environment and consider the OMIEC, together with the electrolyte and gate electrode, as a complete system.

History of OMIEC design for OECTs

The first OECTs were built in the mid-1980s with the introduction of the conducting polymers polypyrrole[31] and polyaniline[32] as the channel materials (Fig. 1b). However, these materials' limited performance and vulnerability to oxidation curtailed their broader applications. In 1990, the synthesis of poly(3,4-ethylenedioxythiophene) (PEDOT) with the water-soluble counterion poly(styrene sulfonate) (PSS) marked a pivotal breakthrough in electronically conducting polymers[33]. The hole-transporting (p-type) films cast from PEDOT:PSS dispersion in water exhibited attributes such as high conductivity, stability, transparency and biocompatibility and, thus, quickly gained prominence in various industrial and research fields[34–36]. One of the most successful utilizations of PEDOT:PSS is in the OECT technology[37], primarily because of its unique microstructure that is beneficial for mixed conduction: the presence of a PSS-rich phase in the film allows for ion and water uptake, surrounding interconnected PEDOT-rich regions which transport electronic charges[38].

However, PEDOT:PSS does have certain limitations. Because it exists in its doped state at zero gate voltage owing to the fixed PSS^- anions inside the film, the OECTs operate in 'depletion' mode. Although the depletion mode affords a high g_m value at low operating potentials, the device has low transconductance efficiency (g_m obtained per unit current) and high power demand, and its use in integrated circuit design is not straightforward. Its high capacitance in the 'off' state restricts the available options for the gate electrode selection. Additionally, synthetic modification of PEDOT:PSS to fine-tune its properties for targeted applications has been very challenging, if not impossible, which limits the areas that OECTs can expand to.

Advances in OECT technology require new, readily tuneable materials, particularly ones that are intrinsically non-conductive and can be operated in enhancement mode. To this end, in 2014, a sulfonated polythiophene derivative (PTHS) was used in an OECT channel, resulting in a high-g_m enhancement mode device[39]. Terminating the alkyl side chain with an ionic unit renders the polythiophene a mixed conductor (that is, known as a conjugated polyelectrolyte), facilitating ion infiltration and ion motion in the film bulk, without the need for a separate ion-conducting phase, as is the case for PEDOT:PSS. A pioneering work in 2016 has demonstrated the feasibility of operating OECTs with

Box 1

Electrochemical doping—coupling between ionic and electronic charges

In an organic mixed ionic–electronic conductor (OMIEC), the electronic charge exists ideally only in the presence of a stabilizing ion with the opposite polarity. This coupling between ionic and electronic charges — commonly referred to as electrochemical or bulk doping — enhances the electrical conductivity of the otherwise low-conductivity OMIEC film. Electrochemical doping is achieved through the presence of dopant ions within the film. Whereas some materials (such as poly(3,4-ethylenedioxythiophene):poly(styrene sulfonate) (PEDOT:PSS)) are designed to encapsulate these charge-stabilizing dopants, others withdraw them when an electrical field is applied through the interfacing electrolyte and become temporarily conducting. The removal of these ions initiates the dedoping process. In the absence of an externally applied potential, an equilibrium concentration of electronic and ionic charges exists, determined by the energetic position of the molecular orbitals of the OMIEC, the nature of the electrolyte and the work functions of contact electrodes. The extent of coupling between electronic charges and ionic charges can be tuned by the applied voltage or other stimuli that can trigger ion uptake (or release). The voltage applied through the electrolyte injects ions into multiple locations inside the film, accessing various electronic sites. Different conducting states can be achieved by adjusting the bias strength. This phenomenon is reflected as a potential-dependent volumetric capacitance (C*), quantified by measuring the amount of ionic charge injected per unit voltage per volume of the OMIEC.

conventional p-type backbones through the introduction of glycolated side chains[40]. By replacing alkylated conjugated polymers with oligoether side chains, hydration and ion penetration were enhanced, shifting the operation mode from an electrical double layer into volumetric electrochemical doping. Researchers have embraced the design principle of integrating hydrophilic side chains into conjugated backbones, including electron-transporting (n-type) films, leading to a rapid evolution of OECT materials over the subsequent years (Fig. 1b). Starting in 2017, the community began utilizing the product of C^* and μ_{OECT} (instead of g_m, which is device geometry-dependent) as figure of merit to compare the performance of various OMIECs[26–28].

In 2018, the ladder-type conjugated polymer poly(benzimidazobenzophenanthroline) (BBL) was introduced to the field of OECTs[41]. The exceptional performance of BBL as an OMIEC is surprising, as the polymer does not contain hydrophilic side chains. Its ability to operate in an OECT channel with such high performance was attributed to three factors: the rigid extended system in BBL induces high μ; the absence of solubilizing chains generates a high polaron density, resulting in a large C*; and the inherent free volume generates nano-voids, which act as ion-permeable regions[42].

Despite the complexity of establishing definitive design rules for OMIECs, a few key principles have been proposed[28,43–46]. The forthcoming section outlines some of these principles, used in a synthetic work aiming to develop high-μC^* OMIECs using various building blocks (see Fig. 2 for common chemical motifs) — although, as we will see in the following sections, other material functionalities become more important for certain applications (see Fig. 3 for representative OMIECs in applications), and a high μC^* alone might not be sufficient. This discussion focuses on polymeric (conjugated) mixed conductors, as they are the most widely used materials in OECT applications. Organic small-molecule semiconductors also have the ability to couple and transport electronic and ionic charges across OECT-relevant distances[47–52]. However, creating a film structure based on small molecules, which maintains connectivity while allowing volumetric ion uptake and release at low biases, is more challenging, despite some advantages they may offer.

OMIEC library and design considerations

The synthetic design of the OMIEC backbone has a profound impact on the energetics of the film, determining factors such as the voltage range leading to distinct electronic states, and the interactions and reactions with oxygen (O_2), water and common molecular species in the biological operating conditions, such as hydrogen peroxide (H_2O_2). The energetics influence the OECT threshold voltage (V_{TH}) and operation range, as well as its stability and reactivity. It is the chemical structure that largely determines the film microstructure, which affects the μC^* product, hence the device performance.

Owing to the efforts in the field of organic electronics, synthetic chemists have a broad understanding of how different motifs in polymer backbones, chain lengths and their distributions contribute to the electronic transport properties. However, unlike the highly ordered polymer chain packing required for high mobility, which is the most important consideration for field-effect transistors, OMIECs need to allow sufficient space for ions to get close to the polymer backbone for high capacitance. Therefore, when designing OMIECs, aspects that influence crystalline and amorphous content of the film become equally important, as they collectively govern the speed and number of ionic and electronic charge couples. This point highlights the importance of side chain architecture in OMIEC design because it not only promotes ion motion in the film but also influences electronic conduction by changing how the chains stack in the solid state and determining the film viscoelasticity during device operation.

The design of backbone units in OMIECs determines the dominant charge carrier type transporting in the film, such as p-type (most common), n-type (fewer examples) and ambipolar (hole and electron conductor, the least common). The p-type OMIECs are constructed from electron-rich (donating) fragments and include polythiophenes and their polyelectrolyte-based homopolymers (Fig. 2a), all-donor polymers (Fig. 2b), and donor–acceptor (D–A) polymers (Fig. 2c). Conversely, n-type polymers are composed of electron-deficient (withdrawing) moieties. We classify n-type OMIECs into three categories: imide-based or lactam-based polymers, including those based on naphthalenediimide (NDI), bithiophene imide (BTI), diketopyrrolopyrrole (DPP) and azaisoindigo (AIID) (Fig. 2d); ladder-type polymers, including BBL and poly(benzodifurandione) (Fig. 2e); and isoindigobenzodifurandione (IID-BDF)-based polymers that are composed of polylactam or polylactone (Fig. 2f).

To obtain ambipolar OMIECs, a unique energetic structure with a low band gap (≤1 eV) is required to achieve the balance between hole and electron mobility[53]. The typical examples of ambipolar OMIECs are shown in Fig. 2g (refs. 54–56). However, owing to their

tendency to localize in a relatively large band gap, constructing ambipolar OMIECs with high and balanced ambipolar properties remains challenging. In this regard, blending p-type and n-type materials in a bulk-heterojunction structure (Fig. 2h) is an effective strategy to enable the transport of both charge carriers and broaden their versatility[57,58]. Matched performance can be achieved by tuning the blend ratios of p-type and n-type material.

Oligoether-based side chains and those containing ionic units such as sulfonates, carboxylic acids, hydroxylates and lysins are commonly used in OMIECs (Fig. 2). Studies revealed that a high polar content in the film increased C^* but also swelling, adversely decreasing μ owing to the disrupted film morphology upon voltage-induced ion uptake and release[59,60]. Even the distribution of ethylene glycol (EG) units along the backbone was found to influence hydration, which led to differences in device performance[61]. One approach to reduce excess swelling is to introduce comonomers with hydrophobic alkyl side chains into the structure[62–64]. Another approach is to add spacers to increase the separation between the oxygen atoms of the oligoether side chains and the conjugated backbone[65–67]. This approach minimizes detrimental swelling near the conjugated backbone, enhancing substrate adhesion and enabling reversible redox reactions, all while improving mobility in aqueous electrolytes[62,63]. Atomistic modifications of the carbon and oxygen within the side chain can tune the microstructure and swelling properties of the OMIEC (refs. 68,69). When propylene glycol and butylene glycol were used as side chains, the increase in hydrophobicity decreased water infiltration. The concomitantly increased crystallinity in the structure is thought to create kinetic barriers that impede oxygen diffusion, minimizing the electrochemical side reactions[70]. The relationship between polar unit content, swelling and packing structure is still not entirely clear, and further research is needed to establish these design guidelines.

p-Type OMIECs

A crucial aspect of OMIEC backbone design is the energetics. Even minor modifications within the OMIEC backbone can have a substantial impact on the frontier molecular orbital energies, arising from factors such as electron delocalization through aromatic ring resonance and/or planarity, the introduction of electron-withdrawing or electron-donating substituents, and the alteration of intermolecular interactions[71]. To achieve high-transductance p-type OECTs, it is essential to select OMIEC building blocks that generate a sufficiently shallow highest occupied molecular orbital (HOMO) level. A shallow HOMO, which can be approximated to the ionization potential of a polymer, translates into a low V_{TH} in OECTs. V_{TH} represents the minimum V_G required to modulate the channel current; hence, it is one of the most important device merits. A shallow HOMO allows for the doping of the polymer within the electrochemical potential window of water, which ranges from 4.05 eV (H^+/H_2 reduction) to 5.30 eV (H_2O/O_2 oxidation) at pH = 7 (ref. 72). Approaches to achieving a shallow HOMO level are to introduce substituents that facilitate lone-pair donation from heteroatoms or to extend the conjugation length through coplanarity-enhancing non-covalent interactions[28]. For instance, the positioning of EG side chains near the heterocyclic structural units of the backbone can create conformational locking between oxygen and sulfur atoms, thereby promoting coplanarity. A well-known example of p-type OMIECs is based on a thiophene backbone, specifically an all-donor polymer composed of thiophene and thiophene derivatives (thienothiophene (TT), bithiophene (T2) and/or alkylenedioxythiophene)[73–75] with an EG side chain. By manipulating the comonomers and altering the regio-positioning of the side chains on the bithiophene units, three resulting polymers, g2T-T (ref. 76), poly(2-(3,3′-bis(2-(2-(2-methoxyethoxy)ethoxy)ethoxy)-[2,2′-bithiophen]-5)yl thiophene) (p(g2T-TT))[40] and poly(2-(4,40-bis(2-methoxyethoxy)-50-methyl-[2,20bithiophen]-5-yl)-5-methylthieno[3,2-b]thiophene) (pgBTTT)[77], exhibit planarizing effects through O–S interactions. This strategy leads to a shallow HOMO level (≥−4.61 eV), with pgBTTT demonstrating a high p-type mobility of 3.44 $cm^2 V^{-1} s^{-1}$.

The p-type OMIEC materials are typically susceptible to spontaneous doping by oxygen, which leads to high currents prior to biasing. Lowering the HOMO level ≤−4.9 eV can minimize the faradaic side reactions with oxygen. To tune the electrochemical properties and minimize unwanted side reactions with oxygen in ambient conditions, whose byproducts can affect the stability of p-type OMIECs and limit their shelf lifetime, electron acceptors are frequently introduced into thiophene-based backbones to construct D–A configuration. For example, DPP and isoindigo serve as acceptors that can be combined with strong donors such as T2, glycolated thienylenevinylene (gTVT) or bis(3,4-ethylenedioxythiophene) to build D–A polymers, such as p(gTDPP-T2) (ref. 78), PIBET-AO (ref. 65) and TDPP-gTVT (ref. 79), respectively. The film stability is also associated with polaron distribution, which can be controlled by backbone modification. For instance, the inclusion of methoxybithiophene unit into polymer p((gPyDPP-MeOT2) provides enhanced delocalization of the wavefunction for the hole polaron compared with the T2 unit. The result is a stable hole polaron, increasing redox cycling stability of the OMIEC (ref. 80).

In addition to molecular design, the purification of polymer needs to be considered. Residual palladium (Pd) traps charges and acts as a co-catalyst for oxygen reduction reaction (ORR), worsening OMIEC stability. Removing this residual resulted in the current top p-type OECT performer, p(g4T2-TT), with a μC^* of 2,008 F V^{-1} cm^{-1} s^{-1} and enhanced stability[81].

n-Type OMIECs

The development of n-type OECTs has been difficult with long-standing challenges extending beyond OMIECs. The lower performance of n-type compared with p-type transistors is mostly attributed to electrochemical side reactions occurring within the film, particularly with oxygen (ORR)[82].

To ensure thermodynamic stability and control the overpotentials of ORR, a deep-lying LUMO level below −4.0 eV is necessary[72]. Therefore, one strategy to enhance the performance, as well as the stability, of n-type OMIECs is to deepen the LUMO level, minimizing electron loss to water and oxygen. The desired LUMO energy levels are commonly achieved by introducing more electron-deficient building blocks, such as NDI, DPP, AIID, BTI and lactam–lactone units.

For instance, the first reported glycolated n-type OMIEC is a copolymer consisting of glycolated NDI and bithiophene units, known as p(gNDI-g2T). NDI was chosen as the backbone component owing to its low-lying LUMO level, ease of modification, and stability. NDI-based materials have since been extensively optimized through side chain modifications, backbone engineering and chemical dopants[54,60,66,83]. By adding new chemistries to the NDI unit while keeping the LUMO requirement as a standing stone, the performance has notably advanced, as evidenced by the progression with μC^* from 0.18 F cm^{-1} V^{-1} s^{-1} to 2.31 F cm^{-1} V^{-1} s^{-1} (refs. 84,85.) These improvements primarily arose from the enhanced mobility rather than the C^* increase. However, although NDI-based materials are widely used in

p-Type OMIECs

a Thiophene-based homopolymer

PTHS

P3MEEMT

b All-donor type

p(g2T-TT)

g2T-T

pgBTTT

c Donor–acceptor type

p(gPyDPP-MeOT2)

p(gDPP-T2)

PIBET-AO

TDPP-gTVT

n-Type OMIECs

d Imide-based and lactam-based

p(gNDI-gT2)

f-BTI2g-TVTCN

P(gTDPP2FT)

gAIID-2FT

e Ladder type

BBL

PBFDO

f IID-BDF-based

p(g$_7$NC$_{10}$N)

p(N-T)

p(C2F-V)

Ambipolar OMIECs

g Single component

2DPP-OD-TEG

p(C$_4$-T2-Cy-EG)

PNDIODTEG-2Tz

PNDI2TEG-2Tz

h Blend

PrC$_{60}$MA

p(g2T-TT)

BBL

PBBTL

Fig. 2 | Chemical structures of representative OMIECs. Chemical structures of representative p-type organic mixed ionic–electronic conductors (OMIECs): thiophene-based homopolymers (part **a**), all-donor type (part **b**) and donor-acceptor type (part **c**). Chemical structures of n-type OMIECs: imide-based and lactam-based (part **d**), ladder-type (part **e**) and isoindigobenzodifurandione (IID-BDF)-based (part **f**). Chemical structures of ambipolar OMIECs: single-component (part **g**) and blends of p-type and n-type materials (part **h**). AIID, azaisoindigo; BBL, poly(benzimidazobenzophenanthroline); BTI, bithiophene imide; DPP, diketopyrrolopyrrole; NDI, naphthalenediimide; PBFDO, poly(benzodifurandione); PTHS, poly(6[thiophene-3-yl]hexane-1-sulfonate) tetrabutylammonium; TDPP, thiophene-flanked DPP.

OECT-based biosensors[86] and neurocomputing[56,87,88], the mobility of NDIs remains limited owing to charge carrier confinement within the acceptor moieties and the presence of twisted backbone conformation characterized by sizeable torsional angles between the NDI and the donor moieties.

Alternative electron-deficient acceptors include DPP, AIID and BTI (ref. 89). Typical strategies that use these acceptors involve weakening the donor moieties with functional groups such as difluorothiophene, cyanated bithiophene and cyanated thienylene-vinylene–thienylene, which reduce the LUMO level and enhance the delocalization of the polaron distribution. For instance, introducing electron-withdrawing fluorine and cyano groups to the donor units of the BTI-containing conjugated polymers f-BTI2TEG-FT and f-BTI2g-TVTCN deepened the LUMO levels of the polymers and improved their electron mobilities[90,91]. Incorporating pyrazine-flanked DPP and cyano-functionalized thiophene with branched EG side chains can also enhance mobility. The mobility enhancement in these cases has been associated with enhanced planarity of the backbone and distribution of the negative polaron along the backbone[92].

Thiophene-flanked DPP (TDPP) can be used to construct n-type OMIECs when combined with fluorine-functionalized thiophene (2FT). By balancing charges towards the donor moiety, the polymer P(gDPP2FT) can transition from a p-type state to an n-type state, with a μC^* of 42.2 F cm^{-1} V^{-1} s^{-}1 (ref. 93). Additionally, the AIID unit, with its electron-deficient character and planarity, offers favourable conditions for facile electron injection and n-type operation in the aqueous media[94–96]. An AIID-based D–A polymer incorporating a weakly fluorinated thiophene (gAIID-2FT) exhibited not only high performance but also remarkable operational stability and long ambient shelf-life stability[95]. In addition to the benefits of a deep LUMO level for electron transport, this example demonstrated that reducing water uptake and its associated morphological changes by incorporating hydrophobic fluorine atoms is key to resistance against cycling-related degradation. These findings highlight the considerable potential for developing high-performance OMIECs with relatively simple structures through small atomistic modifications.

IID-BDF-based polymers have strong electron-deficient properties and rigid backbones. One example with a polylactam backbone is PgNaN, which has both alkyl and EG side chains[64]. Several derivatives of PgNaN were obtained by systematically increasing the alkyl chain length from ethyl to hexadecyl[97]. Fine-tuning the regulation of ion diffusion and electron transport through the balance of hydrophobic and hydrophilic characteristics led to the high-performing polymer p(g7NC10N). IID-BDF-type polymers can also be based on polylactone, such as the lactone-based polymer p(N-T) synthesized through metal-free aldol polymerization[98]. The electron-deficient lactone-building blocks allow a low-lying LUMO level and a rigid backbone necessary for efficient electron mobility. Fluorinating and combining the lactone unit with a vinylene bridge locked the backbone of p(C2F-T) and deepened the LUMO level, resulting in an n-type polymer with a μC^* value of 108 F cm^{-1} V^{-1} s^{-1} (ref. 99).

Facets of OMIECs leveraged in OECTs

Charge transport properties

The electrical properties of OMIECs at the electrolyte interface influence device steady state and transient performance and are determined by three key phenomena: ionic–electronic charge coupling, electronic charge transport and ionic charge transport. For efficient electronic charge transport, hence high μ, the material needs to be extensively π-conjugated, which entails loosely bound electrons capable of moving along the delocalized π-orbitals and between molecules with sizeable π–π overlap. However, the presence of disordered domains limits the extent of delocalization and overlap, such that charge transport occurs through a series of thermally activated hops between states that fall within a statistical probability range of distance and energy[100,101]. Efficient electronic transport relies on the careful selection of appropriate repeat units and side chains that promote molecular ordering, chain planarity and sufficient molecular weight to enable interconnectivity between ordered domains. This allows for the formation of percolative paths, enabling efficient macroscopic electrical conductivity. Operando optical microscopy measurements suggest that the heterogeneity in the energetic landscape limits the drift of holes in the channel, leading to slow device switching speeds at a low biasing regime[102,103].

In dry and minimally hydrated OMIEC films, ion motion occurs via ion hopping, coupled with segmental motion of the OMIEC side chains or backbone[2]. When most OMIECs come into contact with solvent or liquid electrolytes, they swell, and the solvated ion transport occurs at an accelerated rate[2]. In some OMIEC systems, proton conduction can occur even more rapidly through the Grotthuss mechanism[104]. This mechanism involves the hopping of protons between hydronium and water molecules within a hydrogen-bonded network. To facilitate ion transport, careful consideration must be given to the molecular weight and chain architecture of the material, aiming to promote segmental motion while avoiding the formation of dense and large crystalline structures that may hinder ion transport. The dynamics of ion motion and doping kinetics can also be controlled through polymer–electrolyte interface modification. To achieve rapid switching, a successful strategy involves utilizing internally ion-gated OECTs, embedded with small mobile ions within the film, which forgoes the need for an external electrolyte and reduces the distance and time required for ion transit[8]. Ionic liquids that permeate the semiconductor before biasing were shown to enhance the device bandwidth[104].

In various applications of OECTs, it is imperative to have efficient charge transport in the OMIEC channel, characterized typically by a high μC^*, while keeping the device speed fast and its V_{TH} low. For instance, the high g_m and the fast switching speed of OECTs bearing the glycolated bithiophene-based p-type polymer p(g1T2-g5T2) enabled the detection of weak abnormal cardiac rhythms with high peak-to-peak amplitude and low noise[105]. The same electrical characteristics of the OMIEC guaranteed high-resolution photoplethysmograph signal acquisition when the OECT was integrated with a photodiode[106]. Large ‘on’ currents and high μC^* of BBL, matching that of the p-type

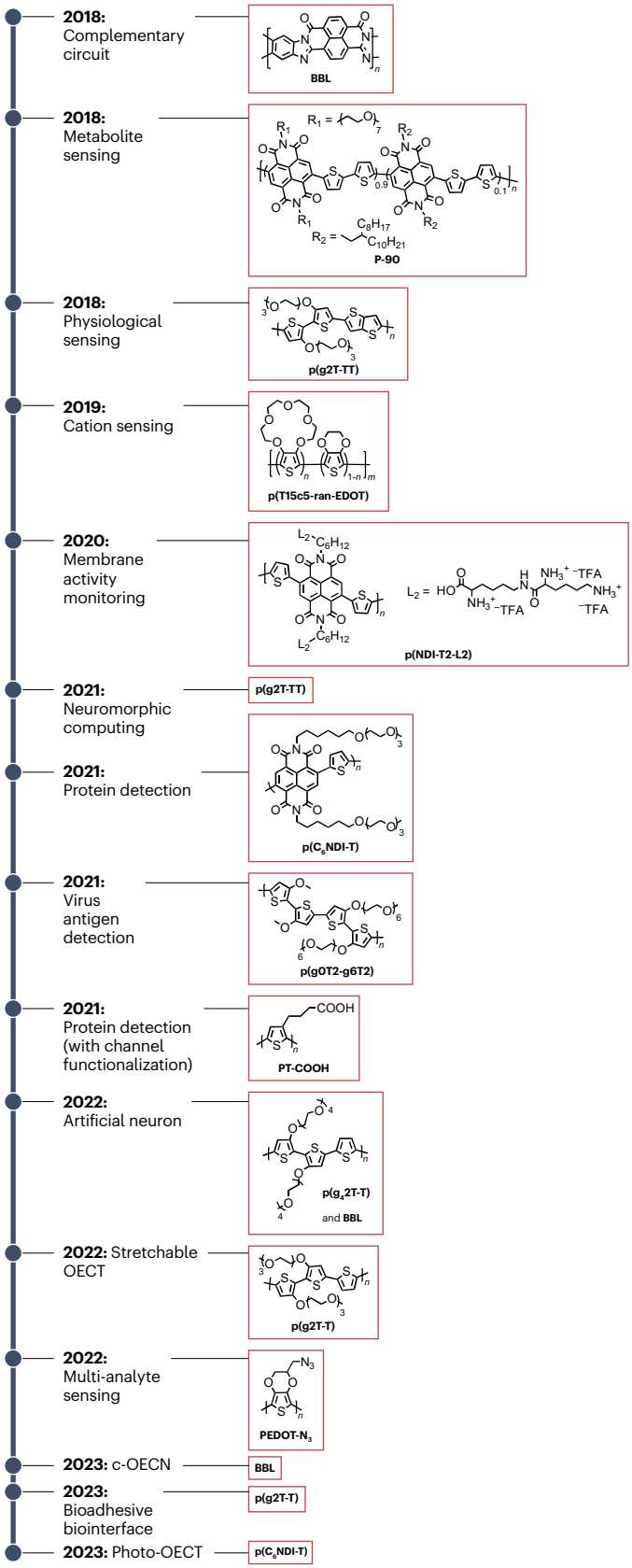

Fig. 3 | Timeline of OMIEC designs. The development timeline of OMIEC designs that have enabled the associated OECT applications. BBL, poly(benzimidazobenzophenanthroline); c-OECN, conductance-based organic electrochemical neuron; NDI, naphthalenediimide; OECT, organic electrochemical transistor; PEDOT, poly(3,4-ethylenedioxythiophene):poly(styrene sulfonate).

analogues, improved further through optimization of its molecular weight[107], allowing the building of all-organic electrochemical complimentary circuits and logic gates[41,58,108]. Such devices can also be constructed by using a single ambipolar OMIEC with equally high μC^* at p-regime and n-regime[55].

Whereas OECTs are typically operated under biasing conditions that maximize the g_m, the subthreshold region operation provides advantages in terms of low power consumption and enhanced sensitivity in various bioelectronic applications. For instance, the p-type glycolated p(g2T-TT) has relatively low 'off' currents before ionic doping starts. The channel current increases exponentially at low V_G, resulting in a high g_m efficiency[109]. This characteristic proves beneficial when using the OECT to detect low-amplitude electrophysiological signals. Similar output characteristics and g_m efficiencies can be attained with other OMIECs that can accept doping ions at low voltages. For example, an OMIEC structurally very similar to p(g1T2-g5T2) enabled very sensitive and low-limit-of-detection protein sensors when the analyte binding-associated OECT signals were evaluated at the subthreshold region[110,111].

It is common to use OECTs to transduce biochemical binding events that change the impedance of the gate electrode. To construct efficient sensors, the device components and geometry should be chosen such that the channel capacitance is close to that of the gate[112,113]. Access to an OMIEC library with various C^* values at different biasing conditions allows an appropriate channel-to-gate capacitance ratio to be achieved without modifying the gate electrode. For instance, the NDI–thiophene-based p(C_6T2) is an n-type polymer with high C^* at low V_G in addition to high g_m. The mobility of this polymer family was enhanced through the inclusion of alkyl spacer atoms on the EG-based chains, moving the polar side chains away from the backbone[54]. A similar NDI-based n-type with alkyl spacers, called p(C_6NDI-T), was used in OECTs to detect amyloid-β protein aggregates and the coronavirus spike protein at concentrations as low as attomolar–femtomolar range owing to the C^* of the channel matching that of the gate electrode[111,114].

The ability to finely tune the OMIEC conductance with external bias and the rapid transition of the film between distinct doping states in response to sub-microsecond voltage pulses have enabled their use in electrochemical random-access memory (ECRAM) devices. However, for integrating these devices into hardware-based artificial neural networks, it is essential for the film to remain in one doping state without the bias for an extended period to enhance long-term memory[56,104]. This can be achieved through synthetic design[70,115] and microstructure optimization[30,116]. One way to improve conductance state retention is increasing the crystallinity of the film, which can suppress the back diffusion of ions[117]. Annealing, for example, can enhance crystallinity, causing ions to become trapped within the ordered and compact side chains. These ions can only be released (de-trapped) when a sufficient potential is applied to overcome the energy barrier, ensuring non-volatility[30] (Fig. 4a). By leveraging the chemical and morphological versatility of organic semiconductors and controlling the rates of ion injection and release, it becomes possible to adjust the write–read speeds of the OECTs. Although p-type OMIECs

show such non-volatility, n-type OECTs may be less suitable for this purpose because ORR deteriorates the retention performance[118]. One solution to this issue involves using vertical architectures wherein the channel is encapsulated with solid electrolytes that prevent air penetration[87].

The ion-dependent switching property of n-type OECTs becomes useful for building an artificial neuromorphic hardware, as it emulates the functionality of spiking neurons. An example is BBL, an OMIEC with conductivity that can be finely tuned by biasing but also decreases upon high electrochemical doping, a property known as anti-ambipolarity[119].

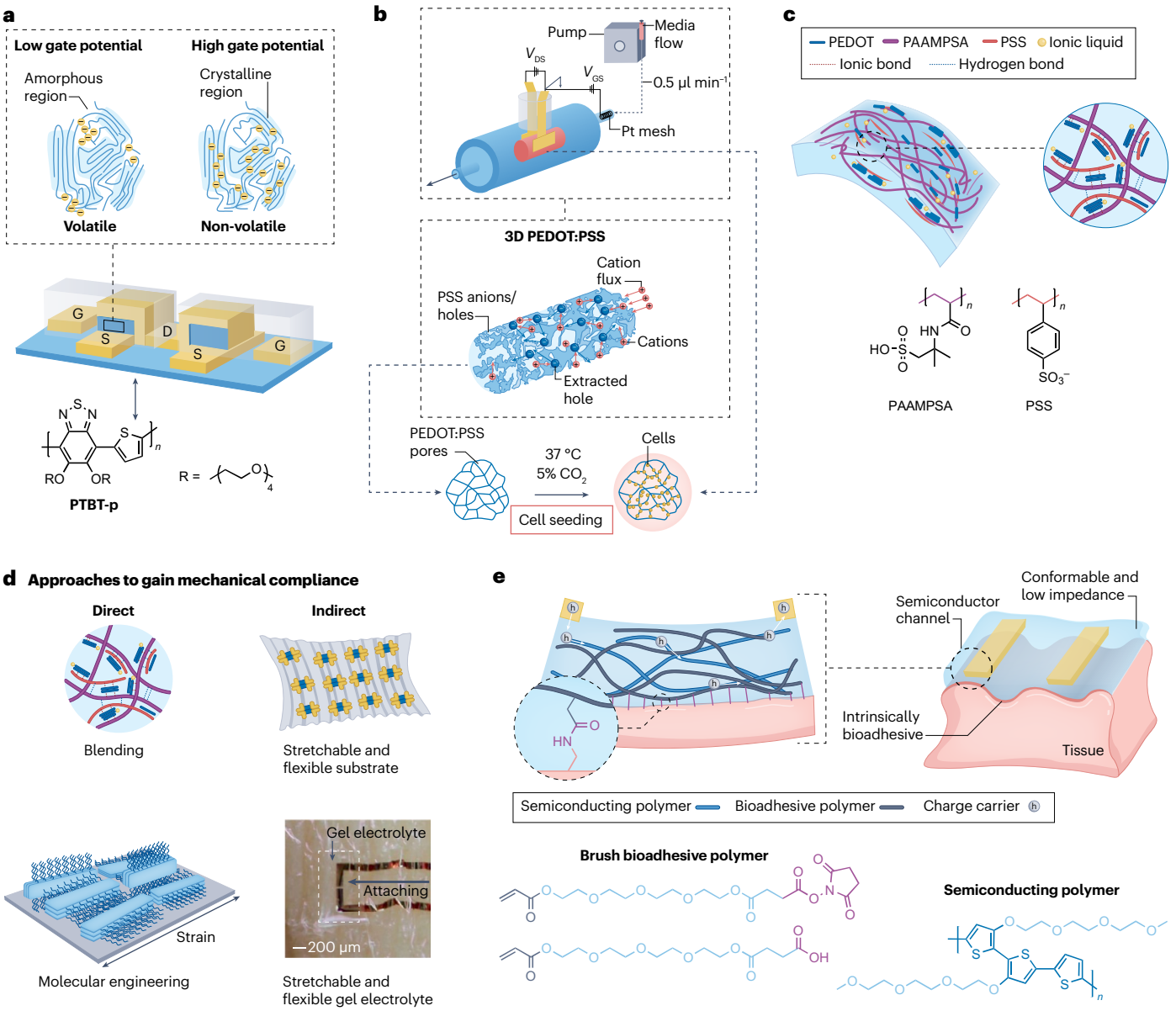

Fig. 4 | Strategies for controlling the electrical and mechanical properties of OECTs. a, Device architecture of the vertical OECT. The ion transport pathways in the volatile or non-volatile mode (top) and the chemical structure of PTBT-p (bottom). **b**, A tubistor, an OECT assembled in a tube embedded with three-dimensional poly(3,4-ethylenedioxythiophene):poly(styrene sulfonate) (PEDOT:PSS) scaffold as the channel, which can be used as an in situ cell culture for tissue development monitoring. **c**, A PEDOT:PSS/PAAMPSA/IL composite comprising of dynamic bond networks (hydrogen bonds, ionic bonds and electrostatic interactions). **d**, Direct approaches to making stretchable OECTs involve blending the semiconducting channel with compliant materials and using molecular engineering. Indirect approaches include using a stretchable substrate and gel-like electrolyte. **e**, An adhesion between an OECT and a wet tissue surface (top) and the chemical structure of the channel composite (bottom). D, drain; G, gate; PAAMPSA, poly(2-acrylamido-2-methyl-1-propanesulfonic acid); S, source. Part **a** reprinted from ref. 30, CC BY 4.0. Part **b** reprinted with permission from ref. 124, AAAS. Parts **c** and **d** adapted with permission from ref. 129, Wiley. Part **d** adapted with permission from ref. 22, Wiley; adapted with permission from ref. 23, Wiley; and reprinted with permission from ref. 131, copyright 2017 American Chemical Society. Part **e** adapted with permission from ref. 142, AAAS.

The ion-tunable polarity of BBL mimics the activation and deactivation of sodium channels in neurons, resulting in a single-material conductance-based complementary organic electrochemical neuron[14]. Through the use of an OMIEC whose conductance is sensitive to biological species or external stimulus, such as light, it becomes possible to construct functional and more biomimetic neuronal networks.

Mechanical properties

Properties such as softness, self-healing, flexibility and stretchability are important for platforms that require mechanical compliance, including wearable and implantable bioelectronics and organ-on-chip type of systems. OMIECs possessing these mechanical traits provide an excellent foundation for OECT-based sensors that detect physiological signals and biochemical substances within their interfacing tissue. These mechanically adaptable OMIECs should also be biocompatible and have structural and operational stability in a biological milieu (essential for wet applications), as well as after strain and deformation cycles[120].

Softness. The softness metrics of OMIECs are tunable and desirable for biological interfacing. Often, OMIECs swell in a biological medium, and their softness increases further. The OMIEC film softness can be increased by the addition of softer components into the polymer casting solution[15], by formulating conductive hydrogels[121,122], or by decreasing the glass transition temperature and/or the degree of crystalline order through molecular design[123]. The polymeric channels with matching mechanical characteristics to the cells can be used to grow cells, allowing the OECT to continuously monitor their integrity and other markers during different stages of tissue development[124] (Fig. 4b). Conversely, for applications that require mechanical robustness, dopants can make films more rigid[20]. The fact that softness is linked to the doping state of the film underpins a possible new application of OMIECs as actuators and pumps.

Self-healing. Self-healing is defined as the ability of the material to recover from physical damage without external intervention. Self-healable semiconducting films in the channel can increase the practicality and shelf life of OECTs as biological sensors. One of the key concepts in self-healing materials is the ability of the fractured conjugated polymer to undergo reversible molecular interactions, and dynamic bonds (such as electrostatic interactions, ionic bonds and hydrogen bonds), either within or between the polymer chains, are often a part of this mechanism[125]. The dynamic bonds in the polymer matrix can break and reform, helping distribute the stress and aiding in the repair of the material. Multiple types of dynamic bonds can be realized by blending conjugated polymers with other soft material matrices (that is, healing agents)[126] or integrating molecular building blocks such as 2,6-pyridine dicarboxamide in the backbone[127] or poly(acetamidoalkyl acrylate) as the side chains[128]. For example, a self-healable OECT was designed using PEDOT:PSS mixed with the healing agent poly(2-acrylamido-2-methyl-1-propanesulfonic acid) (PAAMPSA) that forms hydrogen and ionic bonds with the OMIEC (ref. 129). The hygroscopic PAAMPSA and PEDOT:PSS swell upon mechanical damage, which give the chains mechanical mobility to fill the damaged area and reform the dynamic bonds, as depicted in Fig. 4c. It was possible to increase the segmental chain mobility of PEDOT:PSS with plasticizing agents such as nonionic surfactants[130]. In most cases, however, the self-healing relies on the contact of the damaged area with water or the hydrogel used as the electrolyte. Whether OMIECs other than PEDOT:PSS can be self-healable using similar agents is also unclear.

Stretchability and flexibility. Stretchability describes the capacity of a material to change its dimensions without breaking in response to an applied force. An elastic material will return to its original dimensions once the stretching forces are removed. Flexibility pertains to the ability of a polymer to bend without fracturing when subjected to various types of deformation, including distortion, buckling and twisting, among others. Frequently, stretchability within a polymer matrix is concomitant with its intrinsic flexibility. Stretchable and flexible OECTs can be realized through two primary approaches: (1) adjusting the substrate and the electrolyte and (2) conferring these attributes to the OMIECs by integrating mechanically adaptable elements into the polymer structure or film.

The first approach relies on the use of stretchable or flexible elastomers as the substrate, the insulating layer and the electrolyte to reduce the mechanical failure of the OMIEC channel upon stretching and to maximize the conformability of the device (Fig. 4d). The first stretchable and flexible OECT was developed using a parylene transfer patterning technique to convey the metal contacts and the PEDOT:PSS channel onto a pre-stretched polydimethylsiloxane substrate[131]. A stretchable acrylamide-based hydrogel was cut and pasted on the active area to serve as the electrolyte, and the resulting OECT exhibited consistent and stable transistor characteristics under an applied strain of up to 30%. OECTs using a stretchable glycerol-based gel as a biocompatible polymer matrix for electrolyte ions exhibited a minimal change in the electrical performance under an applied strain of up to 30% (ref. 23). Stretchable OECTs could also be fabricated with biocompatible, biodegradable and all-edible solid-state materials — polysaccharide and choline-based ionic liquid — that served not only as the electrolyte but also as the substrate for the device[132]. Techniques to create stretchable or flexible OECTs include the laser-based patterning[133], microcrack contact electrodes[134], direct-write additive process[17] and screen printing[19]. In these cases, although the OMIECs are not flexible or stretchable, the fact that they can be processed via various methods and integrated with such mechanically variant substrates with minimal loss of conductivity upon moderate mechanical stress highlights the unique compatibility of this material class for stretchable electronics applications.

The second approach for developing flexible and stretchable OECTs focuses on the channel itself. This method aims to improve the transistor durability during repeated usage, acknowledging that if the channel lacks inherent mechanical compliance, mechanical breakdown is inevitable. The mechanical compliance of the channel material can be adjusted through a blend strategy or by fine-tuning the molecular backbone and side chains (Fig. 4d). Incorporating insulating elastomers (such as polystyrene-block-poly(ethylene-ran-butylene)-block-polystyrene (SEBS))[135], hydrogel materials (such as poly(vinyl alcohol), poly(ethylene glycol), poly(vinyl alcohol) and poly(acrylic acid))[136,137], or small molecules that can suppress large aggregate growth[138] with the conjugated polymers can manipulate the film's mechanical properties. Using this blending method, stretchable OECTs have been developed[129,139].

Although these methods confer flexibility and stretchability, they might not present a universal solution. This is because not every OMIEC can be compatible for mixing with these components, or the resultant morphology of the blend can potentially compromise electrochemical properties, given that the added materials typically impede charge transport by disrupting the interconnectivity of conductive network of

OMIECs. Certain chemical design strategies, which have been applied for conventional conjugated polymers, can be useful to synthesize stretchable OMIECs (ref. 140). These include copolymerization with flexible nonconjugated spacers, the introduction of dynamic bonding sites to facilitate non-covalent crosslinking, the incorporation of conjugated rigid fused rings, and the fabrication of conjugated random terpolymers. In addition, side chain engineering has been explored to synthesize stretchable and flexible conjugated polymers, adding features such as nonconjugated flexible side chains, side chains with H-bonding sites, and biaxially extended conjugated side chains. These strategies were able to reduce the persistence length (indicative of rigidity), increase chain mobility and control the crystalline and amorphous domains, promoting reversible strain energy dissipation.

Relatively limited attention has been spent on making OMIECs stretchable and flexible, creating a sizeable opportunity for OECTs. One study has investigated the ability of an OMIEC, p(g2T-T), originally tailored for high μC^* (ref. 76), to withstand strain[22]. The polymer retained its electrical properties even when subjected to 200% strain during 5,000 cycles. The key design features of this OMIEC include a nonlinear backbone architecture, low EG side chain density owing to the unsubstituted thiophene unit, and a high molecular weight (M_n = 67.5 kDa). Another example of a stretchable OECT uses the D–A-type polymer poly(2,5-bis(2-octyldodecyl)-3,6-di(thiophen-2-yl)-2,5-diketo-pyrrolopyrrole-alt-2,5-bis(3-triethyleneglycoloxy-thiophen-2-yl)) (DPP-g2T), with oligoether side chains. The amphiphilicity of the polymer allowed to generate a honeycomb porous structure within a biaxially pre-stretched SEBS substrate, which rendered the device stretchable[141].

OMIECs that combine high stretchability and charge carrier mobility can also be designed to effectively adhere to wet tissue, a crucial aspect for OECT applications that interface directly with it. Blending a bioadhesive brush polymer with an OMIEC in a double-network structure achieved a bioadhesive polymer semiconductor. The brush polymer contained carboxylic acid and *N*-hydroxysuccinimide ester groups that absorb water, which subsequently induced film drying and bolstered adhesion following the initial contact with the tissue[142] (Fig. 4e). Although the innovation lies not solely within the OMIEC itself, the noteworthy aspect is that the semiconductor properties remain unaffected despite blending with a functional material, opening up a new avenue for exploration.

Response to other stimuli

The ability to tune the chemical and physical functionalities of OMIECs is a key feature for successfully integrating OECTs into diverse applications. OMIECs that are responsive to various stimuli, such as biochemical species, pH variations, temperature changes and light exposure, can be designed through chemical modifications or by blending the OMIEC with inherently responsive materials. The latter is accomplished through diverse film fabrication techniques such as freeze drying, sol–gel processes, electrospinning and electropolymerization. The chemical modification strategy involves several avenues, including the synthesis of new monomers, side chain modifications and the post-processing of OMIEC films. Using these strategies considerably expands the design of versatile OMIECs that can react to an array of external stimuli.

For instance, the OMIEC structure can be designed to facilitate the adhesion of specific biomolecules or living cells. Functional derivatives of EDOT are commonly used to enable the conjugation of specific peptides – like integrin-recognized peptide sequences and RGD peptides – on their surfaces, which are recognized by cells[143,144]. Lysine side chains tethered to the dithienyl-diketopyrrolopyrrole and thiophene backbone imitate the extracellular environment of cells, promoting better neuron cell growth on the OMIEC surface[145]. n-Type OMIECs can also be engineered to interact specifically with biomolecules or cells, hence, facilitating a wide range of applications. For instance, integrating hydrophilic side chains allowed to link redox enzymes on the polymer surface, used to build metabolite sensors[146] (Fig. 5a). These specific oligoether-to-alkyl unit ratio of the side chains regulates the interactions of the film with cell membrane components and, thus, influences cell adhesion dynamics[147] (Fig. 5b). Lysine-based side chains on an n-type polymer allowed the formation of a two-dimensional lipid bilayer, through which the activity of a pore-forming protein channel could be monitored[148] (Fig. 5c). Side chain engineering can construct biofouling-resistant OMIEC surfaces, which hinder or minimize non-specific adsorption of molecules and cells[143]. These surfaces can mitigate inflammatory reactions when in contact with tissue, enhancing biocompatibility. The nature of side chains determines surface charge, surface energy and wettability. These factors collectively influence not only the quantity but also the conformation of catalytic enzymes adsorbing on n-type OMIEC surfaces, crucial when building enzymatic metabolite sensors using the OECTs[149].

EDOT-based backbones bearing reactive units offer a means to covalently attach biofunctional units, such as enzymes, antibodies, aptamers and DNA, which selectively bind and react with specific biomolecules. Among these functional monomers are carboxylic acid-functionalized EDOT (EDOT–acid)[144], hydroxymethyl-EDOT (EDOT–OH)[150], amino-modified EDOT (EDOT–NH_2)[151], EDOT derivative bearing an oxyamine moiety (EDOTOA)[152], crown-ether-functionalized EDOT[153] and azidomethyl-EDOT (EDOT–N_3)[154] (Fig. 5d). A 'clickable' OECT utilizing PEDOT–N_3 in the channel has recently been introduced[154]. The azide groups can undergo click reactions with alkyne-bearing molecules including an acetylene–PEG_4–biotin and a dibenzocyclooctyne-modified aptamer for the detection of NeutrAvidin and thrombin, respectively. This method allows control over biomolecule orientation on the film surface. However, it is important to note that synthesizing these functional PEDOT derivatives typically involves electrochemical polymerization, which often necessitates a conducting substrate, if not a channel with a very small length or interdigitated design, and can be challenging to scale up. Other OMIECs that are solution processible and suitable for biofunctionalization are conjugated polyelectrolytes, and an example is polythiophenes with carboxylic acid or hydroxyl groups at the side chain terminals. These units allow for the immobilization of biorecognition units on the OECT channel covalently or via hydrogen bonds, respectively[155]. The antigen–antibody interactions occurring at the OMEIC channel change the potential drop distribution along the electrode, allowing to correlate channel current changes to analyte concentrations.

Multi-functional OECTs can be built directly by blending OMIECs with materials responsive to stimuli such as pH and temperature (Fig. 5e). For instance, PEDOT doped with bromothymol blue dye has been synthesized for pH-sensitive OECTs (ref. 156), whereas blending PEDOT:PSS with a thermoresponsive polymer, specifically poly(*N*-isopropylacrylamide), has enabled a micrometre-scale OECT-based temperature sensor[157].

Most OMIECs are also photoactive owing to their conjugated backbone. As such, light can be another source, in addition to gate biasing, to generate free charge carriers in the transistor if the

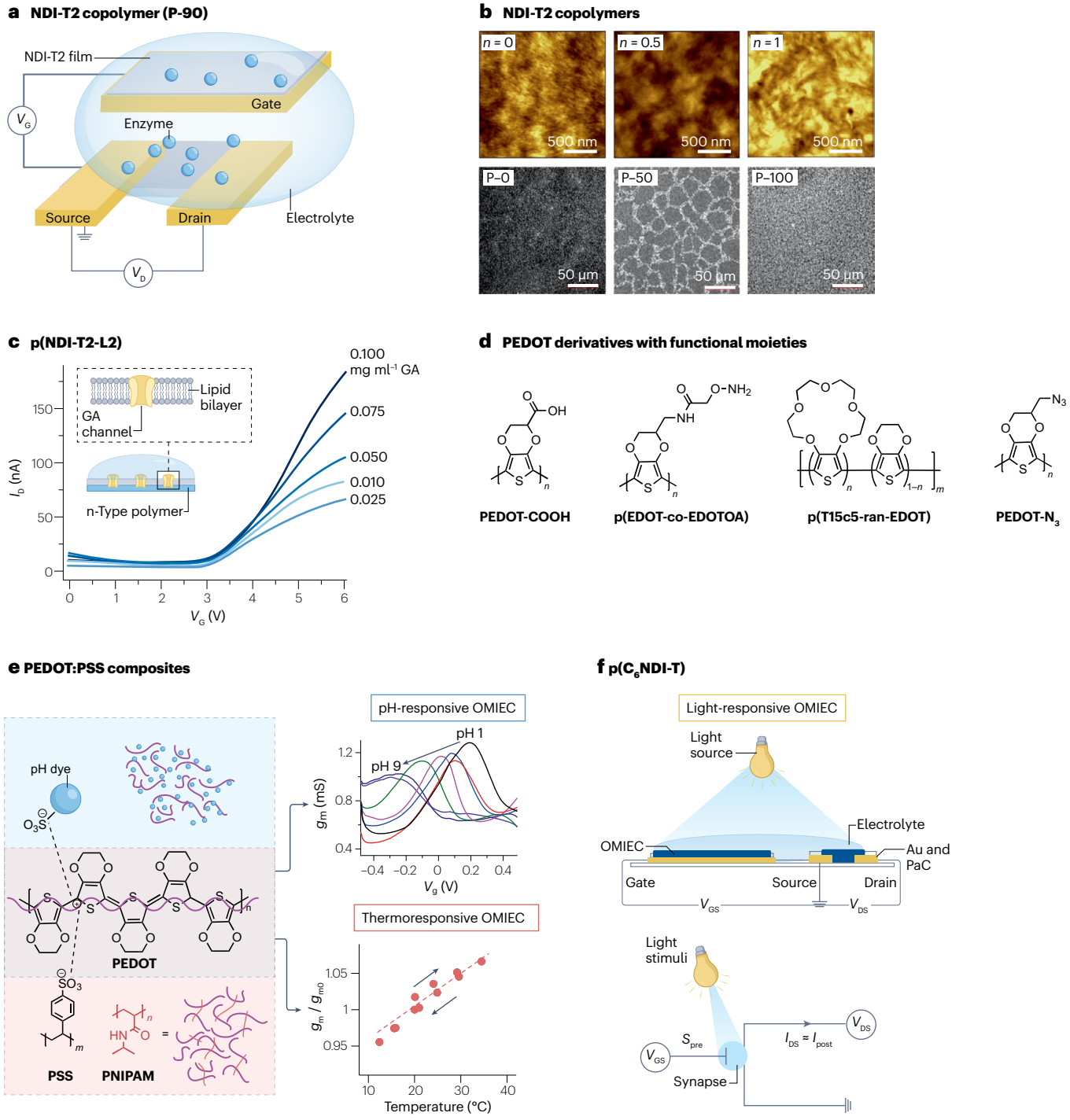

photogenerated excitons can be separated. For example, an n-type photo-electrochemical transistor, based on a naphthalene-1,4,5,8-tetracarboxylic-diimide-thiophene backbone (p(C_6NDI-T)) that exhibits strong absorption in the visible range, was shown to have a current modulated by light[24] (Fig. 5f). The electrochemical potential of the NDI-T film in aqueous media substantially changed under light irradiation, subsequently modulating the transistor characteristics. The transistor under light exposure has a g_m 40 times higher than that in the dark. These devices can be used as photodetectors to detect blood pulses, can be operated in light-gated logic circuits, and can build an artificial retina. Another approach produced a light-responsive OECT that undergoes a reversible modulation of its 'on' current upon irradiation with UV (λ = 365 nm) and visible (λ = 530 nm) light[158]. The channel was made of a semiconducting polythiophene derivative (pgBTTT) blended with a photoswitchable material, spiropyran-decorated ethylene glycol (OEG-SP). The pgBTTT–OEG-SP blend exhibited a shift in ionization energy upon light irradiation, which affected its electrochemical switching ability.

Fig. 5 | Strategies towards multi-functional OMIECs and application examples of stimuli-responsive OECTs. a, Organic electronic conductor (OECT) biosensor, showing the adsorbed enzyme on the glycolated naphthalenediimide (NDI)-T2 film in the channel and the gate electrode. **b**, Atomic force microscopy topography images of NDI-T2 films with various side chains (top row) and fluorescence images of the same films after incubation with lipid vesicles (bottom row). **c**, The transfer curve of a lipid bilayer-integrated p(NDI-T2-L2) OECT shows a change as gramicidin (GA) opens the GA channels integrated into the bilayer. **d**, Poly(3,4-ethylenedioxythiophene) (PEDOT) derivatives with functional groups. From left to right: carboxylic acid, oxyamine moiety, crown ether and azidomethyl. Each functional PEDOT can be further conjugated with other molecules. **e**, Blending PEDOT with responsive materials (such as dyes and thermoresponsive poly(*N*-isopropylacrylamide) (PNIPAM)) can introduce pH response and temperature response. **f**, A light-responsive OECT. A representation of the p(C_6NDI-T) channel generating free electron–hole pairs upon light illumination. This device mimics the functionality of a light-sensitive neuron. OMIEC, organic mixed ionic–electronic conductors. Part **a** reprinted with permission from ref. 146, AAAS. Part **b** adapted with permission from ref. 147, copyright 2018 American Chemical Society. Part **e** (upper right) reprinted with permission from ref. 156, copyright 2018 American Chemical Society. Part **e** (lower right) image courtesy of S. Yamamoto. Part **f** reprinted from ref. 24, CC BY 4.0.

Some OMIECs also exhibit inherent catalytic properties, enabling them to catalyse reduction and oxidation reactions at the solid–electrolyte interface (such as enzymatic reactions, electrochemical oxidation of redox species, and ORR). The electrocatalytic behaviour of OMIECs is influenced by their molecular energy levels and the presence of catalytic sites on the polymer chain. The introduction of different donor units (for example, T2 or MeOT2) copolymerized with pyridine-flanked diketopyrrolopyrrole (PyDPP) in the polymer structure changes the oxidation and reduction onset potentials[80]. This modification subsequently alters the capacity of the polymer to partake in electrochemical redox reactions and defines the range of potentials over which faradaic reactions can occur. The manipulation of the polymer structure allows the redox potential window to be adjusted to precisely suit specific catalytic applications. This will allow to engage the electronic charges generated by various stimuli in electrochemical reactions in the electrolyte. Furthermore, ORR has a notable impact, particularly, on n-type OECT characteristics, as demonstrated by a strong inverse correlation between oxygen content in the media and the 'on' current levels. The oxygen-triggered current generation was observed during metabolite oxidation when the n-type OECT was functionalized with the respective enzyme[118]. The reactivity of the film to oxygen has, therefore, been used to build a metabolite sensor.

Outlook and future perspectives

As the OECT applications continue to grow and expand, so too will the requirements of novel materials with tailored properties. Numerous material properties and functionalities remain to be realized for specific fields. For instance, OECT-based biosensors for in vivo applications and chronic applications in vitro in complex biological media require stable channel materials. It is crucial to extend the operational lifespan of OMIECs for the target application, which can range from minutes for disposable sensors to hours for cell culture-based diagnostics, or months for implantable devices. PEDOT:PSS is currently the only material with demonstrated long-term stability[159], but it lacks chemical versatility and works only within a certain electrochemical range, which may not meet the requirements of the particular application. It is also important to identify the operating regions that render a particular OMIEC device stable, as often full range biasing leads to instabilities. Another requirement for OMIECs interfacing with tissue is compliance to avoid strain damage to itself and traumatizing the target. Although progress in stretchable OECTs appears promising, the challenge lies in the optimization of intrinsic stretchability while maintaining the electrical properties when subjected to mechanical deformation cycles, the improved adhesion between layers on the devices, and the realization of scalable manufacturing of stretchable devices. Conversely, OMIECs, when combined with natural or common-commodity materials, are strong candidates for components of edible diagnostic and therapeutic tools, as well as electronic tags for food distribution chains. To achieve such a high level of tissue compatibility and ease of implantation, soft substrate-free OMIECs can be synthesized directly within the biological environment, turning the tissue itself into conducting matter[18,160]. The efforts then need to focus on how to turn these materials into OECT components, as the conducting polymer alone cannot make a sensitive sensor.

A persisting challenge for any OMIEC technology is the development of air-stable and high-performance n-type materials. Their inherent susceptibility to O_2 and water has complicated their development and exploration, leading to a severely lopsided library of few n-type and predominantly p-type OMIECs. Increasingly creative avenues for improving n-type operation have emerged, including side chain alterations and different monomer configurations, to using ladder and two-dimensional polymer architectures[161]. As encouraging as the accelerating n-type development is, the field first needs to focus on understanding what makes the performance of existing n-types lag behind p-types. Doing so will require more emphasis on stability studies, rather than on reporting figures of merit. Comprehensively understanding the sources of operational instability becomes more important as the OECT applications move from bench to bedside. High-performance n-type OMIECs — only if they are stable enough — can make leaps in biosensing of electron-involving biological reactions or cationic species, as well as in integrated circuit technology or neuromorphic device applications, which requires comparable performance from both p-type and n-type devices.

With the rise in artificial intelligence and neural networks, so too has the OECT field seen growing attention on developing artificial synapses and neuromorphic circuits. Although predominantly based on existing OECT technology, some of these devices should show non-volatile state retention, essential for the realization of long-term memory. For this purpose, OMIECs should retain ionic charges without them diffusing back out of the device in its idle state, something that has predominantly only been implemented using solid electrolytes and ionic liquids. Although some approaches have been proposed to emulate state retention and memory in aqueous media, OMIECs designed to do so without external circuit elements would simplify neuromorphic design and device footprint. In this context, machine learning techniques could be a valuable tool in the design of novel OMIECs, as they have the potential to reduce or even replace existing experimental methodologies and aid in unravelling the structure–functionality relationship[162]. These computational methods enhance our predictive capabilities and identify the chemical motifs and their combinations necessary to realize specific solid-state properties. Additionally, they could provide insights into the behaviour of materials at the biological interface, thus expanding the repertoire of meticulously designed materials for bioelectronics, not only for neuromorphics.

As new OMIECs are developed, their characterization becomes ever more imperative. These characterization techniques need to be in situ to enable accurate and relevant analysis of the structural, morphological, mechanical and compositional aspects of OMIECs during the operation of OECTs. Although existing operando techniques have made considerable progress in probing OMIEC operation, elucidating the intricate structural and mixed transport relationships during device operation in different conditions (electrolyte, gate electrode, geometry)[163,164], achieving further understanding needs increasingly complex in situ characterization techniques. The adaptation of existing techniques, such as X-ray absorption spectroscopy, X-ray photon correlation spectroscopy, infrared spectroscopy and electron microscopy for in situ analysis, although inherently difficult, could prove vital for advancing the characterization of OMIECs in the future. The complex nature of mixed ion–electron transport within the mixed polymer–water network, in which each component interacts with one another, makes probing and understanding it a difficult task. Though some aspects of this complex network of interactions have been amenable to investigation, ion transport remains elusive to this day, with only a handful of studies interrogating its properties through optical means[103]. Worse still, even the quantification of μ and C^* remains unstandardized throughout the field. Hence, it is not uncommon to doubt the reported values[27,28]. The rapid expansion of the OMIEC material library is encouraging for OECTs; however, it is equally important that the techniques used to characterize this growing library continue to be adapted, standardized and re-evaluated to successfully elucidate the structure–property relationships.

A number of challenges in the implementation of OMIECs and their OECTs will need to be overcome. The first issue is the commercial availability of OMIECs. From the initial breakthrough of PEDOT:PSS in 1990, it took around 10 years, until the late 2000s, before it could be purchased off the shelves. Further commercialization of OMIECs might not even be practical during this time: as new and improved materials are being reported constantly, investing in large-scale production and sale of the best material today might mean missing out on a better material tomorrow. From a commercial standpoint, it might make the most sense to wait until material design and synthesis reach a plateau and the top performers become clear. Another challenge concerns the scalability of OECT device fabrication. Currently, OECTs are fabricated by limited-scale photolithography techniques in expensive cleanrooms, but these devices often vary in quality, and their yield heavily depends on the experience of the fabricating user. Although the ease of processability of OMIECs is indeed enticing, OECT fabrication must be optimized and streamlined. Finally, OECTs are often pitted against their inorganic silicon-based counterparts, and the competition between them remains colossal. The industry, although open to innovation, is still often wary of moving away from entrenched technology. Hence, to compete in the market, OECTs need to quickly prove their uniqueness and reliability in specific applications. Once OMIECs and OECTs deliver on their promises, OECT-based technology is bound to become ubiquitous.

Published online: 29 February 2024

References

1. Rivnay, J. et al. Organic electrochemical transistors. *Nat. Rev. Mater*. https://doi.org/10.1038/natrevmats.2017.86 (2018).
2. Paulsen, B. D., Tybrandt, K., Stavrinidou, E. & Rivnay, J. Organic mixed ionic-electronic conductors. *Nat. Mater.* **19**, 13–26 (2020).
3. Rivnay, J. et al. Organic electrochemical transistors with maximum transconductance at zero gate bias. *Adv. Mater.* **25**, 7010–7014 (2013).
4. Ohayon, D. & Inal, S. Organic bioelectronics: from functional materials to next-generation devices and power sources. *Adv. Mater.* **32**, e2001439 (2020).
5. Khodagholy, D. et al. In vivo recordings of brain activity using organic transistors. *Nat. Commun.* **4**, 1575 (2013).
6. Gentile, F. et al. A biomimetic, biocompatible OECT sensor for the real-time measurement of concentration and saturation of ions in plant sap. *Adv. Electron. Mater.* **8**, 2200092 (2022).
7. Deng, Y. et al. A flexible and highly sensitive organic electrochemical transistor-based biosensor for continuous and wireless nitric oxide detection. *Proc. Natl Acad. Sci. USA* **119**, e2208060119 (2022).
8. Spyropoulos, G. D., Gelinas, J. N. & Khodagholy, D. Internal ion-gated organic electrochemical transistor: a building block for integrated bioelectronics. *Sci. Adv.* **5**, 9 (2019).
A study that introduces an OECT design with ions pre-trapped inside the channel, which allows the device to switch on and off rapidly.
9. Ji, X. et al. Mimicking associative learning using an ion-trapping non-volatile synaptic organic electrochemical transistor. *Nat. Commun.* **12**, 2480 (2021).
10. Gkoupidenis, P., Schaefer, N., Garlan, B. & Malliaras, G. G. Neuromorphic functions in PEDOT:PSS organic electrochemical transistors. *Adv. Mater.* **27**, 7176–7180 (2015).
11. Wu, H.-Y. et al. Stable organic electrochemical neurons based on p-type and n-type ladder polymers. *Mater. Horiz.* https://doi.org/10.1039/D3MH00858D (2023).
12. Sarkar, T. et al. An organic artificial spiking neuron for in situ neuromorphic sensing and biointerfacing. *Nat. Electron.* **5**, 774–783 (2022).
13. Harikesh, P. C. et al. Organic electrochemical neurons and synapses with ion mediated spiking. *Nat. Commun.* **13**, 901 (2022).
14. Harikesh, P. C. et al. Ion-tunable antiambipolarity in mixed ion-electron conducting polymers enables biorealistic organic electrochemical neurons. *Nat. Mater.* **22**, 242–248 (2023).
15. Inal, S. et al. Conducting polymer scaffolds for hosting and monitoring 3D cell culture. *Adv. Biosyst.* **1**, 1700052 (2017).
16. Kim, Y. et al. Organic electrochemical transistor-based channel dimension-independent single-strand wearable sweat sensors. *NPG Asia Mater.* **10**, 1086–1095 (2018).
17. Massetti, M. et al. Fully 3D-printed organic electrochemical transistors. *npj Flex. Electron.* https://doi.org/10.1038/s41528-023-00245-4 (2023).
18. Strakosas, X. et al. Metabolite-induced in vivo fabrication of substrate-free organic bioelectronics. *Science* **379**, 795–802 (2023).
19. Zabihipour, M. et al. High yield manufacturing of fully screen-printed organic electrochemical transistors. *npj Flex. Electron.* **4**, 15 (2020).
20. Zokaei, S. et al. Tuning of the elastic modulus of a soft polythiophene through molecular doping. *Mater. Horiz.* **9**, 433–443 (2022).
21. Moro, S. et al. The effect of glycol side chains on the assembly and microstructure of conjugated polymers. *ACS Nano* **16**, 21303–21314 (2022).
A study with scanning tunnelling microscopy images showing the molecular organization of conjugated polymer chains with oligoether side chains.
22. Dai, Y. et al. Stretchable redox-active semiconducting polymers for high-performance organic electrochemical transistors. *Adv. Mater.* **34**, 2201178 (2022).
23. Lee, H. et al. Ultrathin organic electrochemical transistor with nonvolatile and thin gel electrolyte for long-term electrophysiological monitoring. *Adv. Funct. Mater.* **29**, 1906982 (2019).
24. Druet, V. et al. A single n-type semiconducting polymer-based photo-electrochemical transistor. *Nat. Commun.* **14**, 5481 (2023).
25. Bonafè, F., Decataldo, F., Fraboni, B. & Cramer, T. Charge carrier mobility in organic mixed ionic–electronic conductors by the electrolyte-gated Van der Pauw method. *Adv. Electron. Mater*. https://doi.org/10.1002/aelm.202100086 (2021).
26. Inal, S., Malliaras, G. G. & Rivnay, J. Benchmarking organic mixed conductors for transistors. *Nat. Commun.* **8**, 1767 (2017).
27. Ohayon, D., Druet, V. & Inal, S. A guide for the characterization of organic electrochemical transistors and channel materials. *Chem. Soc. Rev.* **52**, 1001–1023 (2023).
A paper that provides a tutorial on OECT characterization.
28. Tropp, J., Meli, D. & Rivnay, J. Organic mixed conductors for electrochemical transistors. *Matter* https://doi.org/10.1016/j.matt.2023.05.001 (2023).
A paper that provides a comprehensive review of OECT materials, design guidelines, and μC* comparison.
29. Huang, W. et al. Vertical organic electrochemical transistors for complementary circuits. *Nature* **613**, 496–502 (2023).
30. Wang, S. et al. An organic electrochemical transistor for multi-modal sensing, memory and processing. *Nat. Electron.* **6**, 281–291 (2023).
31. White, H. S., Kittlesen, G. P. & Wrighton, M. S. Chemical derivatization of an array of three gold microelectrodes with polypyrrole: fabrication of a molecule-based transistor. *J. Am. Chem. Soc.* **106**, 3 (1984).
32. Paul, E. W., Ricco, A. J. & Wrighton, M. S. Resistance of polyaniline films as a function of electrochemical potential and the fabrication of polyaniline-based microelectronic devices. *J. Phys. Chem.* **89**, 7 (1985).
33. Friedrich Jonas, A., Gerhard Heywang, B. G., Werner Schmidtberg, L., Heinze, J. & Dietrich, D. Polythiophenes, process for their preparation and their use. US patent 4,987,042 (1991).
34. Donahue, M. J. et al. Tailoring PEDOT properties for applications in bioelectronics. *Mater. Sci. Eng. R Rep.* https://doi.org/10.1016/j.mser.2020.100546 (2020).
35. Alcácer, L. in *Electronic Structure of Organic Semiconductors* Ch. 9 (IOP Publishing, 2018).

36. Elschner, A., Kirchmeyer, S., Lovenich, W., Merker, U. & Reuter, K. *PEDOT, Principles and Applications of an Intrinsically Conductive Polymer* 1st edn (CRC, 2010).
37. Nilsson, D. et al. Bi-stable and dynamic current modulation in electrochemical organic transistors. *Adv. Mater.* **14**, 51–54 (2002).
38. Rivnay, J. et al. Structural control of mixed ionic and electronic transport in conducting polymers. *Nat. Commun.* **7**, 11287 (2016).
39. Inal, S. et al. A high transconductance accumulation mode electrochemical transistor. *Adv. Mater.* **26**, 7450–7455 (2014).
40. Giovannitti, A. et al. Controlling the mode of operation of organic transistors through side-chain engineering. *Proc. Natl Acad. Sci. USA* **113**, 12017–12022 (2016).
41. Sun, H. et al. Complementary logic circuits based on high-performance n-type organic electrochemical transistors. *Adv. Mater.* https://doi.org/10.1002/adma.201704916 (2018).
42. Surgailis, J. et al. Mixed conduction in an n-type organic semiconductor in the absence of hydrophilic side-chains. *Adv. Funct. Mater.* https://doi.org/10.1002/adfm.202010165 (2021).
A research paper that compares side-chain-bearing and side-chain-free n-type backbones using the same device geometry and methods.
43. Kukhta, N. A., Marks, A. & Luscombe, C. K. Molecular design strategies toward improvement of charge injection and ionic conduction in organic mixed ionic-electronic conductors for organic electrochemical transistors. *Chem. Rev.* **122**, 4325–4355 (2022).
44. Lei, Y., Li, P., Zheng, Y. & Lei, T. Materials design and applications of n-type and ambipolar organic electrochemical transistors. *Mater. Chem. Front.* https://doi.org/10.1039/d3qm00828b (2023).
45. Yu, S., Kousseff, C. J. & Nielsen, C. B. n-Type semiconductors for organic electrochemical transistor applications. *Synth. Met.* https://doi.org/10.1016/j.synthmet.2023.117295 (2023).
46. Wang, Y. & Liu, Y. Insight into conjugated polymers for organic electrochemical transistors. *Trends Chem.* **5**, 279–294 (2023).
47. Bischak, C. G., Flagg, L. Q., Yan, K., Li, C. Z. & Ginger, D. S. Fullerene active layers for n-type organic electrochemical transistors. *ACS Appl. Mater. Interfaces* **11**, 28138–28144 (2019).
48. Liao, H. et al. Efficient n-type small-molecule mixed ion-electron conductors and application in hydrogen peroxide sensors. *ACS Appl. Mater. Interfaces* **14**, 16477–16486 (2022).
49. Duan, J. et al. Highly efficient mixed conduction in n-type fused small molecule semiconductors. *Adv. Funct. Mater.* https://doi.org/10.1002/adfm.202203937 (2022).
50. Duan, J. et al. Electron-deficient polycyclic molecules via ring fusion for n-type organic electrochemical transistors. *Angew. Chem. Int. Ed.* **62**, e202213737 (2023).
51. Duan, J. et al. Highly efficient mixed conduction in a fused oligomer n-type organic semiconductor enabled by 3D transport pathways. *Adv. Mater.* **35**, e2300252 (2023).
52. Parr, Z. S. et al. Semiconducting small molecules as active materials for p-type accumulation mode organic electrochemical transistors. *Adv. Electron. Mater.* https://doi.org/10.1002/aelm.202000215 (2020).
53. Kan, J., Chen, Y., Qi, D., Liu, Y. & Jiang, J. High-performance air-stable ambipolar organic field-effect transistor based on tris(phthalocyaninato) europium(III). *Adv. Mater.* **24**, 1755–1758 (2012).
54. Ohayon, D. et al. Influence of side chains on the n-type organic electrochemical transistor performance. *ACS Appl. Mater. Interfaces* **13**, 4253–4266 (2021).
55. Samuel, J. J. et al. Single-component CMOS-like logic using diketopyrrolopyrrole-based ambipolar organic electrochemical transistors. *Adv. Funct. Mater.* https://doi.org/10.1002/adfm.202102903 (2021).
56. Zhang, Y. et al. High-performance organic electrochemical transistors and neuromorphic devices comprising naphthalenediimide-dialkoxybithiazole copolymers bearing glycol ether pendant groups. *Adv. Funct. Mater.* https://doi.org/10.1002/adfm.202201593 (2022).
57. Stein, E. et al. Ambipolar blend-based organic electrochemical transistors and inverters. *Nat. Commun.* **13**, 5548 (2022).
58. Wu, X. et al. All-polymer bulk-heterojunction organic electrochemical transistors with balanced ionic and electronic transport. *Adv. Mater.* **34**, e2206118 (2022).
59. Savva, A. et al. Balancing ionic and electronic conduction for high-performance organic electrochemical transistors. *Adv. Funct. Mater.* https://doi.org/10.1002/adfm.201907657 (2020).
60. Giovannitti, A. et al. The role of the side chain on the performance of n-type conjugated polymers in aqueous electrolytes. *Chem. Mater.* **30**, 2945–2953 (2018).
61. Moser, M. et al. Side chain redistribution as a strategy to boost organic electrochemical transistor performance and stability. *Adv. Mater.* **32**, e2002748 (2020).
62. Schmode, P. et al. High-performance organic electrochemical transistors based on conjugated polyelectrolyte copolymers. *Chem. Mater.* **31**, 5286–5295 (2019).
63. Szumska, A. A. et al. Reversible electrochemical charging of n-type conjugated polymer electrodes in aqueous electrolytes. *J. Am. Chem. Soc.* **143**, 14795–14805 (2021).
64. Chen, X. et al. n-Type rigid semiconducting polymers bearing oligo(ethylene glycol) side chains for high-performance organic electrochemical transistors. *Angew. Chem. Int. Ed.* **60**, 9368–9373 (2021).
65. Wang, Y. et al. Hybrid alkyl–ethylene glycol side chains enhance substrate adhesion and operational stability in accumulation mode organic electrochemical transistors. *Chem. Mater.* **31**, 9797–9806 (2019).
66. Maria, I. P. et al. The effect of alkyl spacers on the mixed ionic-electronic conduction properties of n-type polymers. *Adv. Funct. Mater.* https://doi.org/10.1002/adfm.202008718 (2021).
67. Tan, E. et al. The role of long-alkyl-group spacers in glycolated copolymers for high-performance organic electrochemical transistors. *Adv. Mater.* **34**, e2202574 (2022).
68. Moser, M. et al. Propylene and butylene glycol: new alternatives to ethylene glycol in conjugated polymers for bioelectronic applications. *Mater. Horiz.* **9**, 973–980 (2022).
69. Onorato, J. W. et al. Side chain engineering control of mixed conduction in oligoethylene glycol-substituted polythiophenes. *J. Mater. Chem. A* **9**, 21410–21423 (2021).
70. Zhao, Y. et al. Side chain engineering enhances the high-temperature resilience and ambient stability of organic synaptic transistors for neuromorphic applications. *Nano Energy* https://doi.org/10.1016/j.nanoen.2022.107985 (2022).
71. Roncali, J. Molecular engineering of the band gap of π-conjugated systems: facing technological applications. *Macromol. Rapid Commun.* **28**, 1761–1775 (2007).
72. Leeuw, D. M. D., Simenon, M. M. J., Brown, A. R. & Einerhand, R. E. F. Stability of n-type doped conducting polymers and consequences for polymeric microelectronic devices. *Synth. Met.* **87**, 7 (1997).
73. Savagian, L. R. et al. Balancing charge storage and mobility in an oligo(ether) functionalized dioxythiophene copolymer for organic- and aqueous-based electrochemical devices and transistors. *Adv. Mater.* **30**, e1804647 (2018).
74. Jones, A. L. et al. Branched oligo(ether) side chains: a path to enhanced processability and elevated conductivity for polymeric semiconductors. *Adv. Funct. Mater.* https://doi.org/10.1002/adfm.202102688 (2021).
75. DiTullio, B. T. et al. Effects of side-chain length and functionality on polar poly(dioxythiophene)s for saline-based organic electrochemical transistors. *J. Am. Chem. Soc.* **145**, 122–134 (2023).
76. Nielsen, C. B. et al. Molecular design of semiconducting polymers for high-performance organic electrochemical transistors. *J. Am. Chem. Soc.* **138**, 10252–10259 (2016).
77. Hallani, R. K. et al. Regiochemistry-driven organic electrochemical transistor performance enhancement in ethylene glycol-functionalized polythiophenes. *J. Am. Chem. Soc.* **143**, 11007–11018 (2021).
78. Moser, M. et al. Polaron delocalization in donor-acceptor polymers and its impact on organic electrochemical transistor performance. *Angew. Chem. Int. Ed.* **60**, 7777–7785 (2021).
79. Wang, Y. et al. The effect of the donor moiety of DPP based polymers on the performance of organic electrochemical transistors. *J. Mater. Chem. C* **9**, 13338–13346 (2021).
80. Giovannitti, A. et al. Energetic control of redox-active polymers toward safe organic bioelectronic materials. *Adv. Mater.* **32**, e1908047 (2020).
81. Griggs, S. et al. The effect of residual palladium on the performance of organic electrochemical transistors. *Nat. Commun.* **13**, 7964 (2022).
82. Usta, H. et al. Design, synthesis, and characterization of ladder-type molecules and polymers. air-stable, solution-processable n-channel and ambipolar semiconductors for thin-film transistors via experiment and theory. *J. Am. Chem. Soc.* **1311**, 23 (2008).
83. Paterson, A. F. et al. Water stable molecular n-doping produces organic electrochemical transistors with high transconductance and record stability. *Nat. Commun.* **11**, 3004 (2020).
84. Chen, J. et al. Backbone coplanarity manipulation via hydrogen bonding to boost the n-type performance of polymeric mixed conductors operating in aqueous electrolyte. *Mater. Horiz.* **10**, 607–618 (2023).
85. Cong, S. et al. Donor functionalization tuning the n-type performance of donor–acceptor copolymers for aqueous-based electrochemical devices. *Adv. Funct. Mater.* https://doi.org/10.1002/adfm.202201821 (2022).
86. Koklu, A. et al. Organic bioelectronic devices for metabolite sensing. *Chem. Rev.* **122**, 4581–4635 (2022).
87. Xie, Z. et al. All-solid-state vertical three-terminal n-type organic synaptic devices for neuromorphic computing. *Adv. Funct. Mater.* https://doi.org/10.1002/adfm.202107314 (2022).
88. Zhang, Y. et al. Adaptive biosensing and neuromorphic classification based on an ambipolar organic mixed ionic-electronic conductor. *Adv. Mater.* **34**, e2200393 (2022).
89. Ding, L. et al. Polymer semiconductors: synthesis, processing, and applications. *Chem. Rev.* **123**, 7421–7497 (2023).
90. Feng, K. et al. Fused bithiophene imide dimer-based n-type polymers for high-performance organic electrochemical transistors. *Angew. Chem. Int. Ed.* **60**, 24198–24205 (2021).
91. Feng, K. et al. Cyano-functionalized n-type polymer with high electron mobility for high-performance organic electrochemical transistors. *Adv. Mater.* **34**, e2201340 (2022).
92. Shi, J. et al. Revealing the role of polaron distribution on the performance of n-type organic electrochemical transistors. *Chem. Mater.* **34**, 864–872 (2022).
93. Li, P., Shi, J., Lei, Y., Huang, Z. & Lei, T. Switching p-type to high-performance n-type organic electrochemical transistors via doped state engineering. *Nat. Commun.* **13**, 5970 (2022).
A study that develops a high-performance n-type OECT material based on a p-type backbone.
94. Parr, Z. S. et al. From p- to n-type mixed conduction in isoindigo-based polymers through molecular design. *Adv. Mater.* **34**, e2107829 (2022).
95. Wang, Y. et al. n-Type organic electrochemical transistors with high transconductance and stability. *Chem. Mater.* **35**, 405–415 (2023).
96. Wang, Y. et al. The chemistry and applications of heteroisoindigo units as enabling links for semiconducting materials. *Acc. Chem. Res.* **53**, 2855–2868 (2020).
97. Marks, A. et al. Synthetic nuances to maximize n-type organic electrochemical transistor and thermoelectric performance in fused lactam polymers. *J. Am. Chem. Soc.* **144**, 4642–4656 (2022).
98. Wang, Y. et al. Green synthesis of lactone-based conjugated polymers for n-type organic electrochemical transistors. *Adv. Funct. Mater.* https://doi.org/10.1002/adfm.202111439 (2022).
99. Wang, Y. et al. Acceptor functionalization via green chemistry enables high-performance n-type organic electrochemical transistors for biosensing, memory applications. *Adv. Funct. Mater.* https://doi.org/10.1002/adfm.202304103 (2023).

100. Tessler, N., Preezant, Y., Rappaport, N. & Roichman, Y. Charge transport in disordered organic materials and its relevance to thin-film devices: a tutorial review. *Adv. Mater.* **21**, 2741–2761 (2009).
101. Coropceanu, V. et al. Charge transport in organic semiconductors. *Chem. Rev.* **107**, 926–952 (2007).
102. Inal, S., Malliaras, G. G. & Rivnay, J. Optical study of electrochromic moving fronts for the investigation of ion transport in conducting polymers. *J. Mater. Chem. C* **4**, 3942–3947 (2016).
103. Keene, S. T. et al. Hole-limited electrochemical doping in conjugated polymers. *Nat. Mater.* **4**, 1121–1127 (2023).
104. Melianas, A. et al. Temperature-resilient solid-state organic artificial synapses for neuromorphic computing. *Sci. Adv.* **6**, eabb2958 (2020).
105. Wu, X. et al. High performing solid-state organic electrochemical transistors enabled by glycolated polythiophene and ion-gel electrolyte with a wide operation temperature range from −50 to 110 °C. *Adv. Funct. Mater.* **33**, 2209354 (2023).
106. Zhong, Y. et al. An organic electrochemical transistor integrated photodetector for high quality photoplethysmogram signal acquisition. *Adv. Funct. Mater.* **33**, 2211479 (2023).
107. Wu, H. Y. et al. Influence of molecular weight on the organic electrochemical transistor performance of ladder-type conjugated polymers. *Adv. Mater.* **34**, e2106235 (2022).
108. Yang, C.-Y. et al. Low-power/high-gain flexible complementary circuits based on printed organic electrochemical transistors. *Adv. Electron. Mater.* **8**, 2100907 (2022).
109. Venkatraman, V. et al. Subthreshold operation of organic electrochemical transistors for biosignal amplification. *Adv. Sci.* **5**, 1800453 (2018).
110. Guo, K. et al. Rapid single-molecule detection of COVID-19 and MERS antigens via nanobody-functionalized organic electrochemical transistors. *Nat. Biomed. Eng.* **5**, 666–677 (2021).
111. Koklu, A. et al. Microfluidic integrated organic electrochemical transistor with a nanoporous membrane for amyloid-β detection. *ACS Nano* **15**, 8130–8141 (2021).
112. Liang, Y. et al. Highly sensitive detection of malaria biomarker through matching channel and gate capacitance of integrated organic electrochemical transistors. *Biosens. Bioelectron.* **242**, 115712 (2023).
113. Nissa, J., Janson, P., Berggren, M. & Simon, D. T. The role of relative capacitances in impedance sensing with organic electrochemical transistors. *Adv. Electron. Mater.* **7**, 2001173 (2021).
114. Koklu, A. et al. Convection driven ultrarapid protein detection via nanobody-functionalized organic electrochemical transistors. *Adv. Mater.* **34**, 2202972 (2022).
115. Zhao, Y. et al. Donor engineering tuning the analog switching range and operational stability of organic synaptic transistors for neuromorphic systems. *Adv. Funct. Mater*. https://doi.org/10.1002/adfm.202205744 (2022).
116. Gumyusenge, A., Melianas, A., Keene, S. T. & Salleo, A. Materials strategies for organic neuromorphic devices. *Annu. Rev. Mater. Res.* **51**, 47–71 (2021).
A paper that outlines guidelines for how to design conjugated polymers with memory behavior.
117. Go, G.-T. et al. Achieving microstructure-controlled synaptic plasticity and long-term retention in ion-gel-gated organic synaptic transistors. *Adv. Intell. Syst.* **2**, 2000012 (2020).
118. Druet, V. et al. Operation mechanism of n-type organic electronic metabolite sensors. *Adv. Electron. Mater.* **8**, 2200065 (2022).
119. Xu, K. et al. On the origin of Seebeck coefficient inversion in highly doped conducting polymers. *Adv. Funct. Mater.* **32**, 2112276 (2022).
120. Bai, J., Liu, D., Tian, X. & Zhang, S. Tissue-like organic electrochemical transistors. *J. Mater. Chem. C* **10**, 13303–13311 (2022).
A paper that reviews the advances of OECTs for cutaneous applications.
121. Feig, V. R., Tran, H., Lee, M. & Bao, Z. Mechanically tunable conductive interpenetrating network hydrogels that mimic the elastic moduli of biological tissue. *Nat. Commun.* **9**, 2740 (2018).
122. Keate, R. L., Tropp, J., Serna, C. & Rivnay, J. A collagen-conducting polymer composite with enhanced chondrogenic potential. *Cell. Mol. Bioeng.* **14**, 501–512 (2021).
123. Onorato, J., Pakhnyuk, V. & Luscombe, C. K. Structure and design of polymers for durable, stretchable organic electronics. *Polym. J.* **49**, 41–60 (2017).
124. Pitsalidis, C. et al. Transistor in a tube: a route to three-dimensional bioelectronics. *Sci. Adv.* **4**, eaat4253 (2018).
125. Wang, S. & Urban, M. W. Self-healing polymers. *Nat. Rev. Mater.* **5**, 562–583 (2020).
126. Li, Y., Zhou, X., Sarkar, B., Gagnon-Lafrenais, N. & Cicoira, F. Recent progress on self-healable conducting polymers. *Adv. Mater.* **34**, 2108932 (2022).
A paper that provides a review of self-healing conducting polymers and their OECTs.
127. Oh, J. Y. et al. Intrinsically stretchable and healable semiconducting polymer for organic transistors. *Nature* **539**, 411–415 (2016).
128. Voorhaar, L. et al. Self-healing polythiophene phenylenes for stretchable electronics. *Eur. Polym. J.* **105**, 331–338 (2018).
129. Su, X. et al. A highly conducting polymer for self-healable, printable, and stretchable organic electrochemical transistor arrays and near hysteresis-free soft tactile sensors. *Adv. Mater.* **34**, 2200682 (2022).
130. Ko, J., Wu, X., Surendran, A., Muhammad, B. T. & Leong, W. L. Self-healable organic electrochemical transistor with high transconductance, fast response, and long-term stability. *ACS Appl. Mater. Interfaces* **12**, 33979–33988 (2020).
131. Zhang, S. et al. Patterning of stretchable organic electrochemical transistors. *Chem. Mater.* **29**, 3126–3132 (2017).
132. Jo, Y. J. et al. Biocompatible and biodegradable organic transistors using a solid-state electrolyte incorporated with choline-based ionic liquid and polysaccharide. *Adv. Funct. Mater.* **30**, 1909707 (2020).
133. Marchiori, B., Delattre, R., Hannah, S., Blayac, S. & Ramuz, M. Laser-patterned metallic interconnections for all stretchable organic electrochemical transistors. *Sci. Rep.* **8**, 8477 (2018).
134. Matsuhisa, N. et al. High-transconductance stretchable transistors achieved by controlled gold microcrack morphology. *Adv. Electron. Mater.* **5**, 1900347 (2019).
135. Xu, J. et al. Highly stretchable polymer semiconductor films through the nanoconfinement effect. *Science* **355**, 59–64 (2017).
136. Li, P., Sun, K. & Ouyang, J. Stretchable and conductive polymer films prepared by solution blending. *ACS Appl. Mater. Interfaces* **7**, 18415–18423 (2015).
137. Tseng, Y.-T. et al. Morphology and properties of PEDOT:PSS/soft polymer blends through hydrogen bonding interaction and their pressure sensor application. *J. Mater. Chem. C* **8**, 6013–6024 (2020).
138. Xu, J. et al. Tuning conjugated polymer chain packing for stretchable semiconductors. *Adv. Mater.* **34**, 2104747 (2022).
139. Li, Y., Zhang, S., Li, X., Unnava, V. R. N. & Cicoira, F. Highly stretchable PEDOT:PSS organic electrochemical transistors achieved via polyethylene glycol addition. *Flex. Print. Electron.* **4**, 044004 (2019).
140. Zheng, Y., Zhang, S., Tok, J. B. H. & Bao, Z. Molecular design of stretchable polymer semiconductors: current progress and future directions. *J. Am. Chem. Soc.* **144**, 4699–4715 (2022).
A paper that provides a comprehensive review outlining polymer design guidelines for stretchable electronics.
141. Chen, J. et al. Highly stretchable organic electrochemical transistors with strain-resistant performance. *Nat. Mater.* **21**, 564–571 (2022).
142. Li, N. et al. Bioadhesive polymer semiconductors and transistors for intimate biointerfaces. *Science* **381**, 686–693 (2023).
143. Zhu, B. et al. Large enhancement in neurite outgrowth on a cell membrane-mimicking conducting polymer. *Nat. Commun.* **5**, 4523 (2014).
144. Povlich, L. K. et al. Synthesis, copolymerization and peptide-modification of carboxylic acid-functionalized 3,4-ethylenedioxythiophene (EDOTacid) for neural electrode interfaces. *Biochim. Biophys. Acta Gen. Subj.* **1830**, 4288–4293 (2013).
145. Du, W. et al. Improving the compatibility of diketopyrrolopyrrole semiconducting polymers for biological interfacing by lysine attachment. *Chem. Mater.* **30**, 6164–6172 (2018).
146. Pappa, A. M. et al. Direct metabolite detection with an n-type accumulation mode organic electrochemical transistor. *Sci. Adv.* **4**, eaat0911 (2018).
147. Zhang, Y. et al. Visualizing the solid–liquid interface of conjugated copolymer films using fluorescent liposomes. *ACS Appl. Bio Mater.* **1**, 1348–1354 (2018).
148. Kawan, M. et al. Monitoring supported lipid bilayers with n-type organic electrochemical transistors. *Mater. Horiz.* **7**, 2348–2358 (2020).
149. Ohayon, D. et al. Interactions of catalytic enzymes with n-type polymers for high-performance metabolite sensors. *ACS Appl. Mater. Interfaces* **15**, 9726–9739 (2023).
150. Wustoni, S. et al. In situ electrochemical synthesis of a conducting polymer composite for multimetabolite sensing. *Adv. Mater. Technol.* **5**, 1900943 (2020).
151. Ouyang, L. et al. Enhanced PEDOT adhesion on solid substrates with electrografted P(EDOT-NH2). *Sci. Adv.* **3**, e1600448 (2017).
152. Hai, W. et al. Specific recognition of human influenza virus with PEDOT bearing sialic acid-terminated trisaccharides. *ACS Appl. Mater. Interfaces* **9**, 14162–14170 (2017).
153. Wustoni, S. et al. Membrane-free detection of metal cations with an organic electrochemical transistor. *Adv. Funct. Mater.* **29**, 1904403 (2019).
154. Fenoy, G. E. et al. "Clickable" organic electrochemical transistors. *JACS Au* **2**, 2778–2790 (2022).
155. Song, Y., Wagner, J. & Katz, H. E. The behavior of carboxylated and hydroxylated polythiophene as bioreceptor layer: anti-human IgG and human IgG interaction detection based on organic electrochemical transistors. *Electrochem. Sci. Adv.* **2**, e2100166 (2022).
156. Mariani, F., Gualandi, I., Tessarolo, M., Fraboni, B. & Scavetta, E. PEDOT: dye-based, flexible organic electrochemical transistor for highly sensitive pH monitoring. *ACS Appl. Mater. Interfaces* **10**, 22474–22484 (2018).
157. Kindaichi, S., Matsubara, R., Kubono, A., Yamamoto, S. & Mitsuishi, M. Preparation of resilient organic electrochemical transistors based on blend films with flexible crosslinkers. Preprint at https://doi.org/10.26434/chemrxiv-2023-zztqm (2023).
158. Turetta, N. et al. A photo-responsive organic electrochemical transistor. *J. Mater. Chem. C* **11**, 7982–7988 (2023).
159. Dijk, G., Rutz, A. L. & Malliaras, G. G. Stability of PEDOT:PSS-coated gold electrodes in cell culture conditions. *Adv. Mater. Technol.* https://doi.org/10.1002/admt.201900662 (2019).
160. Inal, S. Turning tissues into conducting matter. *Science* **379**, 758–759 (2023).
161. Wang, M. et al. Exceptionally high charge mobility in phthalocyanine-based poly(benzimidazobenzophenanthroline)-ladder-type two-dimensional conjugated polymers. *Nat. Mater.* **22**, 880–887 (2023).
162. Schmidt, J., Marques, M. R. G., Botti, S. & Marques, M. A. L. Recent advances and applications of machine learning in solid-state materials science. *npj Comput. Mater.* **5**, 83 (2019).

163. Wu, R., Matta, M., Paulsen, B. D. & Rivnay, J. Operando characterization of organic mixed ionic/electronic conducting materials. *Chem. Rev.* **122**, 4493–4551 (2022).
164. Lyu, D. et al. Operando NMR electrochemical gating studies of ion dynamics in PEDOT:PSS. *Nat. Mater.* **22**, 746–753 (2023).

Acknowledgements
This publication is based upon work supported by KAUST Research Funding (KRF) under award numbers ORA-2021-CRG10-4650 and ORA-2021-CRG10-4668, and KAUST Smart Health Initiative under award number REI/1/5130-01-01.

Author contributions
S.I. conceived the project and outlined the manuscript. S.I., Y.W. and S.W. wrote the manuscript and prepared the figures with contributions from Y.Z., J.S. and A.K. All authors reviewed and/or edited the manuscript and figures before submission.

Competing interests
The authors declare no competing interests.

Additional information
Peer review information *Nature Reviews Materials* thanks Howard Katz and the other, anonymous, reviewer(s) for their contribution to the peer review of this work.